JOC The Journal of Organic Chemistry

Article

pubs.acs.org/joc

Probing the Radialene-Character in Triplesalophen Ligands by Spectroscopic and Structural Analysis

Carl-Georg Freiherr von Richthofen, Anja Stammler, Hartmut Bögge, and Thorsten Glaser*

Lehrstuhl für Anorganische Chemie I, Fakultät für Chemie, Universität Bielefeld, Universitätsstr. 25, D-33615 Bielefeld, Germany

Supporting Information

ABSTRACT: The triplesalen ligand system based on three salen-like coordination environments bridged by a common phloroglucinol ring has been designed and successfully applied for the rational synthesis of single-molecule magnets from two trinuclear triplesalen complexes and one hexacyanometallate by supramolecular recognition. In order to optimize this system with respect to magnetic anisotropy, the triplesalophen ligand system has been identified, which should allow for the synthesis of nonanuclear complexes composed of two trinuclear triplesalophen complexes and three connecting units. Herein, the convergent synthesis of the triplesalophen ligand system is described, which differs fom the divergent strategy for the triplesalen ligand system. The molecular and elecrtronic structures of the triplesalophen ligands H_6baron^R (R = Me, Cl, Br) have been established by single-crystal X-ray diffraction, NMR, FTIR, and UV−vis spectroscopies. These complementary methods allowed the assignment of the central compartment not to be in the O-protonated tautomer but in the N-protonated tautomer with the prevalence of a keto-enamine resonance description, which resembles a heteroradialene. Furthermore, the comparison with the mononucleating unsymmetrical salophen reference ligand H_2carl^{Cl} and with compounds from the literature provides unique signatures for the appearance of the heteroradialene motif not only in NMR spectra and structural parameters but also in IR and UV−vis spectra. These signatures form the basis for the interpretation and understanding of the electronic structures of transition metal complexes with the triplesalophen ligand system.

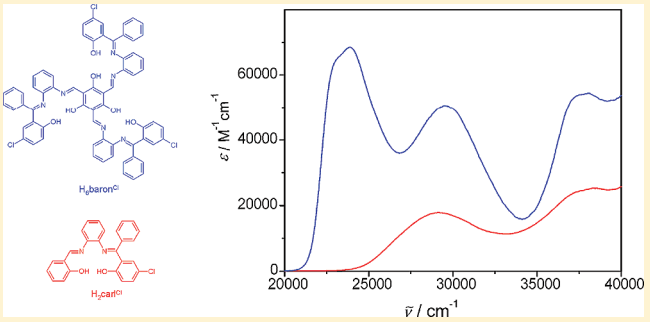

INTRODUCTION

We have designed the triplesalen ligand system[1−3] (Scheme 1) to meet two necessary (but not sufficient) requirements for the rational design of single-molecule magnets (SMMs): (1) a high spin ground state S_t and (2) a strong magnetic anisotropy D_{S_t}. We have chosen the phloroglucinol bridging unit **X** (Scheme 1) to transmit ferromagnetic interactions in trinuclear complexes[4−10] by the spin-polarization mechanism.[11−24] We have chosen a salen-like coordination environment because the salen ligand **Y** (Scheme 1) should establish a pronounced magnetic anisotropy by its strong ligand field in the basal plane.[25−27] A well-studied example is the Jacobson catalyst [(salen′)Mn^{III}Cl] (with H_2salen′ = (*R*,*R*)-*N*,*N*′-bis(3,5-di-*tert*-butylsalicylidene)-1,2-cyclohexanediamine), which is a Mn^{III} (S = 2) species with a strong magnetic anisotropy parametrized by a zero-field splitting parameter D = −2.5 cm^{-1}.[28−30] Severe ligand foldings have been observed in the complexes of the ligand $H_6talen^{t\text{-}Bu_2}$ (= 2,4,6-tris{1-[2-(3,5-di-*tert*-butylsalicylaldimino)-2-methylpropylimino]-ethyl}-1,3,5-trihydroxybenzene) resulting in overall bowl-shaped molecular structures (Scheme 1, bottom left).[2,6] We have taken advantage of this ligand folding by using the trinuclear complexes $[(talen^{t\text{-}Bu_2})\{M^t(solv)_n\}_3]^{m+}$ to act as molecular building blocks with hexacyanometallates $[M^c(CN)_6]^{3-}$ for the formation of heptanuclear complexes $[\mathbf{M^t_6M^c}]^{n+}$ (= $[\{(talen^{t\text{-}Bu_2})M^t\}_3\{M^c(CN)_6\}]^{n+}$): $[\mathbf{Mn^{III}_6Cr^{III}}]^{3+}$,[31] $[\mathbf{Mn^{III}_6Fe^{III}}]^{3+}$,[32] and $[\mathbf{Mn^{III}_6Co^{III}}]^{3+}$[33] with $[\mathbf{Mn^{III}_6Cr^{III}}]^{3+}$ being a single-molecule magnet.

Although $[\mathbf{Mn^{III}_6Cr^{III}}]^{3+}$ exhibits a high spin ground state of S = 21/2, a magnetic anisotropy of the spin ground state, and a molecular C_3 symmetry, the single-molecule magnet properties (anisotropy barrier and blocking temperature) are not better than the first reported SMM $[Mn_{12}O_{12}(O_2CCH_3)_{16}(OH_2)_4]$, $\mathbf{Mn_{12}}$.[34−36] Lately, some strategies have been successful in increasing the blocking temperature in the family of $\mathbf{Mn_6}$ (= $[Mn_6O_2(sao^R)_6(O_2CR')_2(solv)_n]$; with H_2sao = salicylaldoxime) complexes[37−42] and in $\mathbf{Dy_2}$[43] and $\mathbf{Tb_2}$[44] (= [K(18-crown-6)(THF)$_2$][{[(Me$_3$Si)$_2$N]$_2$(THF)Ln}$_2$(μ-η^2:η^2-N_2)]; with Ln = Dy, Tb). We have analyzed the magnetic properties of $[\mathbf{Mn^{III}_6Cr^{III}}]^{3+}$ in detail and identified several optimization strategies.[3] One reason for the low blocking temperature is the too small magnetic anisotropy of the total spin ground state S_t. The main component of the magnetic anisotropy of the total spin ground state arises from the projection of the single-site anisotropies onto the total spin ground state, while dipolar and anisotropic interactions yield mainly only minor contributions.[25,45] In the heptanuclear complexes $[\mathbf{M^t_6M^c}]^{n+}$ the single-site anisotropy tensors of the Mn^{III} ions (which coincides with

Received: November 9, 2011
Published: January 5, 2012

Scheme 1

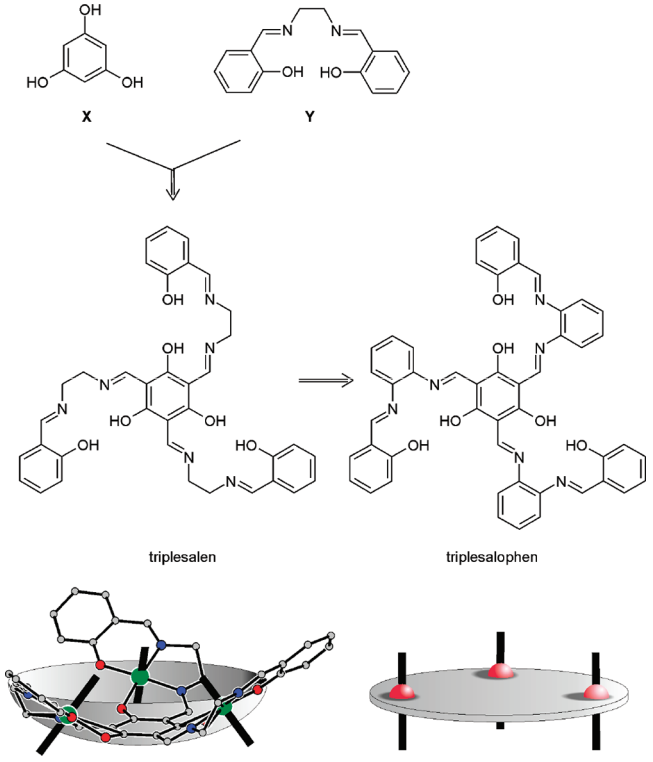

the Jahn–Teller axis indicated by the thick bars in Scheme 1, bottom) are not collinear with the molecular C_3 axis but form angles of 36–41° (Scheme 1, bottom left). This results in an almost cancellation of the local magnetic anisotropies by the projection onto the total spin ground state. A collinear arrangement of the Mn^{III} anisotropy tensors would maximize the projection of the local anisotropies onto the total spin ground state. Thus, an improvement for our system would be an almost planar trinuclear building block (Scheme 1, bottom right) compared to the bowl-shaped triplesalen building block (Scheme 1, bottom left).[2,6] Therefore, the triplesalophen ligand system with a completely sp^2-hybridized and therefore almost planar backbone (Scheme 1) appeared to us as a natural choice for a rational improvement of our system. Trinuclear triplesalophen complexes should thus allow the construction of nonanuclear complexes $[\mathbf{M}^t_6\mathbf{M}^c_3]^{n+}$ with all local anisotropies tensors arranged collinear for maximizing the total magnetic anisotropy instead of the almost cancellation of the local anisotropy tensors in the bowl-shaped heptanuclear complexes $[\mathbf{M}^t_6\mathbf{M}^c]^{n+}$ with triplesalen complexes.

Herein, we present the efficient synthesis of the triplesalophen ligands H_6baron^R (R = Me, Cl, Br; Scheme 2). We have recently communicated the synthesis of H_6baron^{Br} and its trinuclear Ni^{II} complex $[(baron^{Br})Ni\{Ni(py)_2\}_2]$, which exhibits ferromagnetic interactions between the octahedrally coordinated Ni^{II} ions.[46] The specific requirements of the phenylenediamine backbone prevented the application of the established divergent synthesis of the triplesalen ligands. Thus, a convergent synthesis was established. Additionally, the characterization of H_6baron^R in the solid state by high resolution single-crystal X-ray diffraction and in solution by extensive NMR spectroscopy allows a detailed description of the tautomeric and electronic structure of H_6baron^R. In contrast to simple salophen ligands, the triplesalophen ligands H_6baron^R

Scheme 2

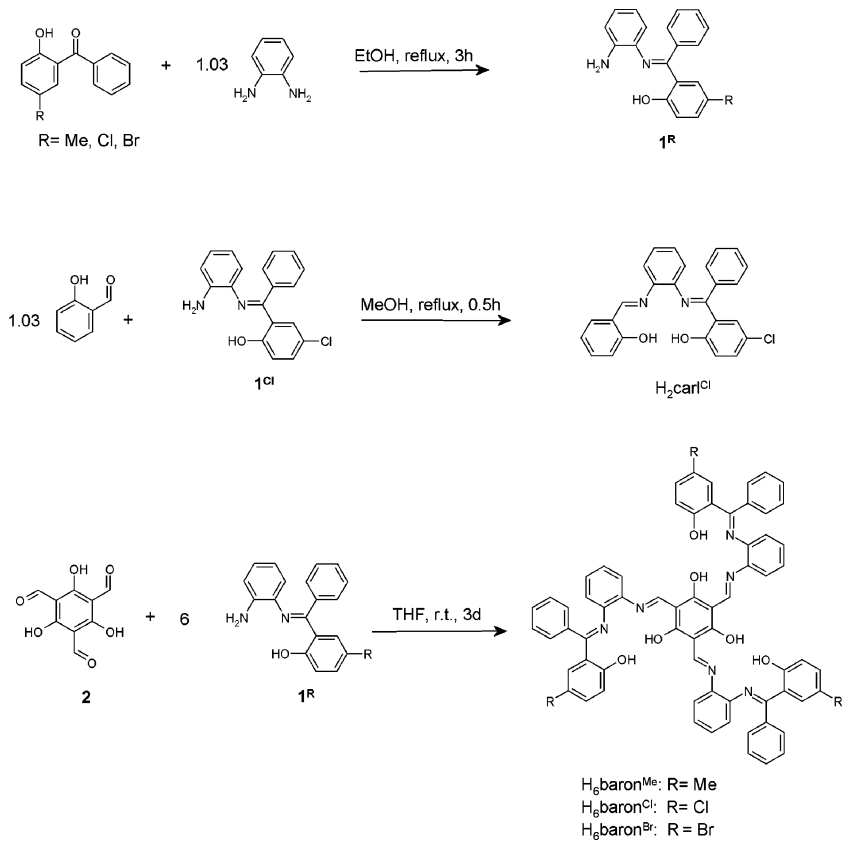

dx.doi.org/10.1021/jo202273s | J. Org. Chem. 2012, 77, 1435–1448

prevail in the N-protonated tautomer in the central backbone with a radialene-like resonance structure ("heteroradialene") being more important than an aromatic benzene resonance structure.

The combined application of the complementary methods NMR spectroscopy, single-crystal X-ray diffraction, FTIR, and UV−vis spectroscopies allowed us to identify prominent signatures of the central heteroradialene in extended phloroglucinol ligands in all four methods. These signatures will allow us the assignment of the electronic structure of the central phloroglucinol backbone in the transition metal complexes with the triplesalophen ligand system.

RESULTS

Synthesis. The syntheses of symmetrical salen ligands are easily achieved by one-pot Schiff-base condensations of one diamine and two identical aldehyde or ketone derivatives. In contrast, the preparation of asymmetrical salen ligands is more challenging and requires a stepwise protocol. In the first step, the isolation of a monocondensed diamine derivative, a so-called half-unit, is necessary.[47−56] The reaction of the remaining amine function of this intermediate with an other aldehyde or ketone derivative would lead to the desired unsymmetrical salen ligand. As imine condensations are equilibrium reactions, the back reaction reforms the first used aldehyde or ketone and the diamine so that a mixture of compounds can be formed. Thus, it is important to consider that an aldimine is usually easy to prepare but not very stable. Ketimines require harsher conditions for the preparation but are usually more stable than aldimines.[57] Therefore, in the first step of the reaction sequence for an unsymmetrical salen ligand, the more stable ketimine half-unit should be synthesized, which reacts with an aldehyde in the second step.

Taking these considerations into account, we were able to prepare the triplesalen ligand system in a divergent synthesis.[1,2] As the isolation of the parent salen half-unit is not feasible,[48] we made use of an observation of Elias and co-workers to isolate the ketimine triplesalen half-unit **A** (Scheme 3).[58] The sterically more crowded amine function of 1,2-diamino-2-methylpropane reacts only with aldehydes but not with ketones.

Beside this half-unit **A** we were also able to synthesize the chiral half-unit **B** of the H_6chand ligand system by using the chiral *trans*-1,2-cyclohexanediamine.[59,60] The isolation of half-unit **B** based on the symmetrical cyclohexanediamine is in accord with the isolation of an analogous salen half-unit[49−51] and may be attributed to the less strong reactivity of cyclohexanediamine. Analogously, we tried to synthesize the triplesalophen ligand system in a divergent synthesis. However, many efforts to synthesize an analogous triplesalophen half-unit **C** (Scheme 3) with the symmetric 1,2-phenylenediamine resulted only in impure solids. Reactions of these solids with salicylaldehyde resulted in the sublimation of the pure symmetrical salophen ligand. Therefore, we tried a convergent approach for the triplesalophen ligand system rather than the established divergent approach for the triplesalen ligand system. This requires a ketimine salophen half-unit and the trialdehyde of phloroglucinol.

Sinn and co-workers established the synthesis of the ketimine salophen half-unit $\mathbf{1}^{Cl}$ (Scheme 2) using 5-chloro-2-hydroxybenzophenone and 1,2-phenylenediamine in the presence of piperidine and triethylorthoformate in ethanol.[61] Thus, we synthesized in the first step the ketimine half-units $\mathbf{1}^{R}$ by a modified procedure of $\mathbf{1}^{Cl}$ and reacted these in a second Schiff-base condensation with trialdehyde **2**[62] in tetrahydrofuran (Scheme 2). The ligands H_6baron^{R} (R = Me, Cl, Br) precipitate

Scheme 3

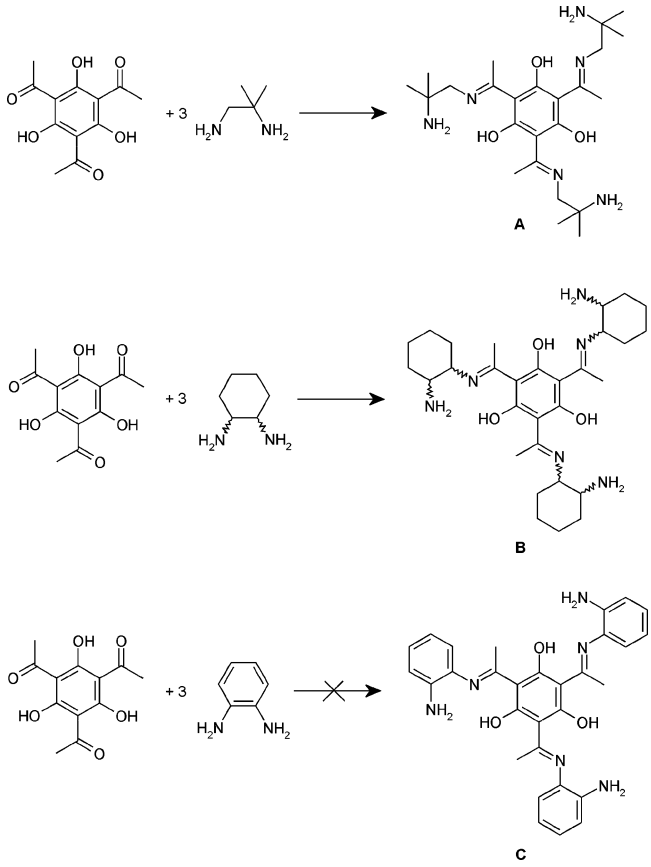

from the reaction solutions as bright yellow solids. As a reference for the comparison of the electronic and structural properties of the unsymmetrical trinucleating triplesalophen ligands with that of an analogous unsymmetrical mononucleating salophen ligand, we also synthesized the ligand H_2carl^{Cl} (Scheme 2). Mass spectrometry and elemental analysis confirmed the successful synthesis of all compounds.

Crystal and Molecular Structures. Crystals of H_2carl^{Cl} suitable for single-crystal X-ray diffraction were obtained by slow diffusion of pentane into a solution of H_2carl^{Cl} in toluene. Selected interatomic distances are summarized in Table 1. The molecular structure of H_2carl^{Cl} (Figure 1) shows that the benzene ring of the phenylenediamine backbone and the phenol ring of the aldimine compartment are almost coplanar (torsion angle C11−N11−C13−C14 = 7.4°), whereas the phenol ring of the ketimine compartment is rotated along N12−C18 resulting in a C17−C18−N12−C19 torsion angle of 64.5°. The benzene ring of the ketimine moiety is almost perpendicular to the phenol ring (C192−C191−C19−C102 torsion angle of 113.4°). The mean values of the C−C bond lengths (Table 2) of the phenol ring of the aldimine and ketimine compartment differ not significantly (1.39 and 1.40 Å, respectively). The same holds true for the C−O bond length (1.36 and 1.35 Å, respectively), and both C═N bond lengths are 1.29 Å. However, the C^{ar}−C^{imine} bond length of the aldimine (1.45 Å) is slightly shorter than for the ketimine (1.48 Å).

Crystals of H_6baron^{R}·C_5H_{12} suitable for single-crystal X-ray diffraction could be obtained for all three triplesalophen ligands by slow diffusion of pentane into a solution of the respective ligand in toluene. All three ligands crystallize in the trigonal space group $P\bar{3}$. Interestingly, H_6baron^{Me}·1.5CH_2Cl_2 obtained

dx.doi.org/10.1021/jo202273s | J. Org. Chem. 2012, 77, 1435−1448

Table 1. Selected Interatomic Distances [Å] for $H_6baron^{R}\cdot C_5H_{12}$, $H_6baron^{Me}\cdot 1.5CH_2Cl_2$, and H_2carl^{Cl}

	$H_6baron^{Me}\cdot C_5H_{12}$	$H_6baron^{Me}\cdot 1.5CH_2Cl_2$	$H_6baron^{Cl}\cdot C_5H_{12}$	$H_6baron^{Br}\cdot C_5H_{12}$	H_2carl^{Cl}
C(1)−C(2)	1.459(3)	1.451(3)	1.450(3)	1.457(3)	1.411(2)
C(1)−C(2) #1[a]	1.458(3)	1.456(3)	1.464(3)	1.459(3)	
C(2)−C(1) #2[a]	1.458(3)	1.456(3)	1.464(3)	1.459(3)	
C(2)−C(11)	1.380(3)	1.385(3)	1.382(3)	1.382(3)	1.445(2)
N(11)−C(11)	1.322(3)	1.322(2)	1.323(3)	1.324(3)	1.286(2)
N(11)−C(13)	1.401(3)	1.404(2)	1.399(3)	1.403(3)	1.412(2)
N(12)−C(19)	1.294(3)	1.292(2)	1.292(3)	1.290(3)	1.293(2)
N(12)−C(18)	1.420(3)	1.424(2)	1.423(3)	1.424(3)	1.423(2)
O(11)−C(1)	1.253(3)	1.258(2)	1.255(3)	1.254(3)	1.355(2)
O(12)−C(101)	1.349(2)	1.353(2)	1.345(2)	1.345(3)	1.347(2)
C(13)−C(14)	1.394(3)	1.388(3)	1.395(3)	1.388(3)	1.399(2)
C(13)−C(18)	1.402(3)	1.404(3)	1.403(3)	1.408(3)	1.402(2)
C(14)−C(15)	1.379(3)	1.389(3)	1.382(3)	1.387(3)	1.381(2)
C(15)−C(16)	1.383(4)	1.384(3)	1.383(4)	1.379(4)	1.384(2)
C(16)−C(17)	1.391(3)	1.387(3)	1.395(3)	1.391(4)	1.384(2)
C(17)−C(18)	1.385(3)	1.385(3)	1.380(3)	1.378(3)	1.394(2)
C(19)−C(102)	1.472(3)	1.467(3)	1.473(3)	1.472(3)	1.476(2)
C(19)−C(191)	1.493(3)	1.493(2)	1.496(3)	1.495(3)	1.496(2)
C(101)−C(106)	1.379(3)	1.380(3)	1.389(3)	1.385(4)	1.397(2)
C(101)−C(102)	1.411(3)	1.411(3)	1.415(3)	1.413(3)	1.418(2)
C(102)−C(103)	1.398(3)	1.403(3)	1.404(3)	1.405(3)	1.409(2)
C(103)−C(104)	1.383(3)	1.372(3)	1.373(3)	1.373(3)	1.378(2)
C(104)−C(105)	1.389(3)	1.393(3)	1.386(3)	1.382(4)	1.390(2)
C(105)−C(106)	1.376(3)	1.374(3)	1.377(3)	1.377(4)	1.380(2)
C(191)−C(196)	1.374(4)	1.381(3)	1.370(4)	1.372(4)	1.390(2)
C(191)−C(192)	1.383(4)	1.389(3)	1.386(4)	1.384(4)	1.392(2)
C(192)−C(193)	1.389(4)	1.388(3)	1.392(4)	1.396(5)	1.389(2)
C(193)−C(194)	1.372(6)	1.380(4)	1.362(6)	1.361(6)	1.382(2)
C(194)−C(195)	1.352(6)	1.384(4)	1.349(6)	1.351(6)	1.389(2)
C(195)−C(196)	1.390(4)	1.378(3)	1.392(4)	1.395(5)	1.391(2)
C(1)−C(6)					1.394(2)
C(2)−C(3)					1.405(2)
C(3)−C(4)					1.380(2)
C(4)−C(5)					1.392(2)
C(5)−C(6)					1.383(2)

[a]Symmetry transformations used to generate equivalent atoms: #1, $-y, x-y-1, z$; #2, $-x+y+1, -x, z$.

by evaporation of a dichloromethane solution crystallizes in the same space group. Selected interatomic distances are summarized in Table 1. As the molecules are almost isostructural, the molecular structure of H_6baron^{Me} in crystals of $H_6baron^{Me}\cdot C_5H_{12}$is shown exemplary in Figure 2. Thermal ellipsoid plots for all structures are provided as Figures S5−S8 in the Supporting Information.

The asymmetric units of $H_6baron^{R}\cdot C_5H_{12}$ consist of one-third of the ligand and one-third of a pentane molecule of crystallization, while that of $H_6baron^{Me}\cdot 1.5CH_2Cl_2$ bears also one-third of the ligand but two disordered dichloromethane molecules of crystallization with 1/6 and 1/3 occupancy.

The ligand molecules in crystals of $H_6baron^{R}\cdot C_5H_{12}$ are bowl-shaped with the bottom built up by the phloroglucinol backbone and the wall by the three ketimine compartments (Figure 2b). Three other ligand molecules are acting as a kind of cover (Figure 3a) with their phenylenediamine backbones. A disordered pentane molecule is encapsulated in this closed bowl. The shortest distance between the ligand and the encapsulated solvent is 3.70 Å (C2−C2P) (sum of the van der Waals radii of two carbon atoms 3.40 Å).

In the case of $H_6baron^{Me}\cdot 1.5CH_2Cl_2$ disordered dichloromethane is encapsulated by the same arrangement as described of $H_6baron^{R}\cdot C_5H_{12}$ (Figure 3b). The shortest distances between the ligand and the encapsulated dichloromethane are 3.59 Å (C2−Cl5) and 3.64 Å (C1−Cl3) (sum of van der Waals radii of a carbon and a chlorine atom 3.50 Å). In contrast to the pentane solvate, in $H_6baron^{Me}\cdot 1.5CH_2Cl_2$ an additional dichloromethane molecule is encapsulated by six phenol rings related by a $\bar{3}$ axis (Figure 3c,d). This solvent encapsulation results in 2D double-layers with the hydroxyl groups pointing outside (Figure 3e).

In all four molecular structures the central phloroglucinol ring and the phenylenediamine backbone are almost coplanar, which is an evidence for a strong conjugation. This coplanarity is lost at N12 by rotation along N12−C18 resulting in C17−C18−N12−C19 torsion angles of the terminal ketimine moieties in $H_6baron^{Me}\cdot C_5H_{12}$, $H_6baron^{Cl}\cdot C_5H_{12}$, $H_6baron^{Br}\cdot C_5H_{12}$, and $H_6baron^{Me}\cdot 1.5CH_2Cl_2$ of 81.2°, 78.0°, 80.9°, and 83.3°, respectively. Additionally, the terminal benzene ring is almost perpendicular to the terminal phenol ring by C192−C191−C19−C102 torsion angles of 94.6°, 102.2°, 97.7°, and 94.1° in $H_6baron^{Me}\cdot C_5H_{12}$, $H_6baron^{Cl}\cdot C_5H_{12}$, $H_6baron^{Br}\cdot C_5H_{12}$, and $H_6baron^{Me}\cdot 1.5CH_2Cl_2$, respectively.

Significant differences become apparent by comparing structural parameters of the central and the terminal moiety of the triplesalophen ligands (Table 2). The mean value of the central C−O bond length (1.26 Å) is shorter than the terminal C−O

dx.doi.org/10.1021/jo202273s | J. Org. Chem. 2012, 77, 1435−1448

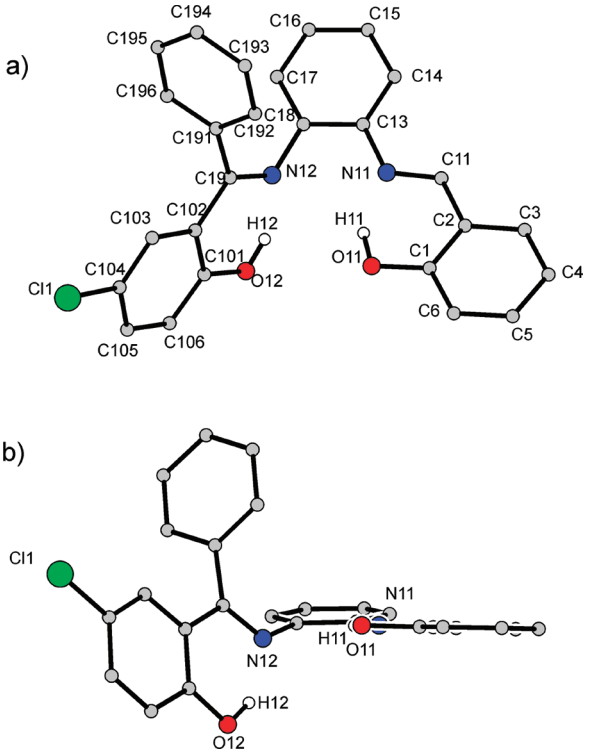

Figure 1. Molecular structure of H_2carl^{Cl} with the numbering scheme used (a) drawn perpendicular to the benzene ring of the phenylenediamine backbone and (b) drawn parallel to the central benzene ring of the aldimine moiety. Hydrogen atoms are omitted for clarity with the exception of H11 and H12.

bond length (1.35 Å). The same effect can be detected for the central and terminal C^{ar}–C^{imine} bond length (1.38 and 1.47 Å, respectively). On the other hand, the mean bond lengths of the central C^{ar}–C^{ar} bond (central, 1.46 Å; terminal, 1.39 Å) and the C=N bond (central, 1.32 Å; terminal, 1.29 Å) are elongated compared to the respective terminal bonds. This tremendous effect is accompanied by a change of the protonation: whereas in the terminal phenol-imine units the phenol oxygen atoms are protonated, the "imine" nitrogen atoms are protonated in the central compartments (Figure 2).

Electronic Absorption Spectroscopy. The electronic absorption spectra of the salophen half-units $\mathbf{1}^{R}$ (Figure 4a) display two broad absorption features at 26700 and 28900 cm^{-1} and higher energy absorption above 35000 cm^{-1} (maximum at: 37300 cm^{-1} for R = Me; 38500 cm^{-1} for R = Cl; 38000 cm^{-1} for R = Br). The electronic absorption spectrum of H_2carl^{Cl} (Figure 4a) exhibits absorption maxima in the same energy range (29100 and 38400 cm^{-1}) but with increased intensity compared to the salophen half-units. The spectra of H_6baron^{R} (R = Me, Cl, Br; Figure 4b) exhibit even stronger absorption features in this energy range

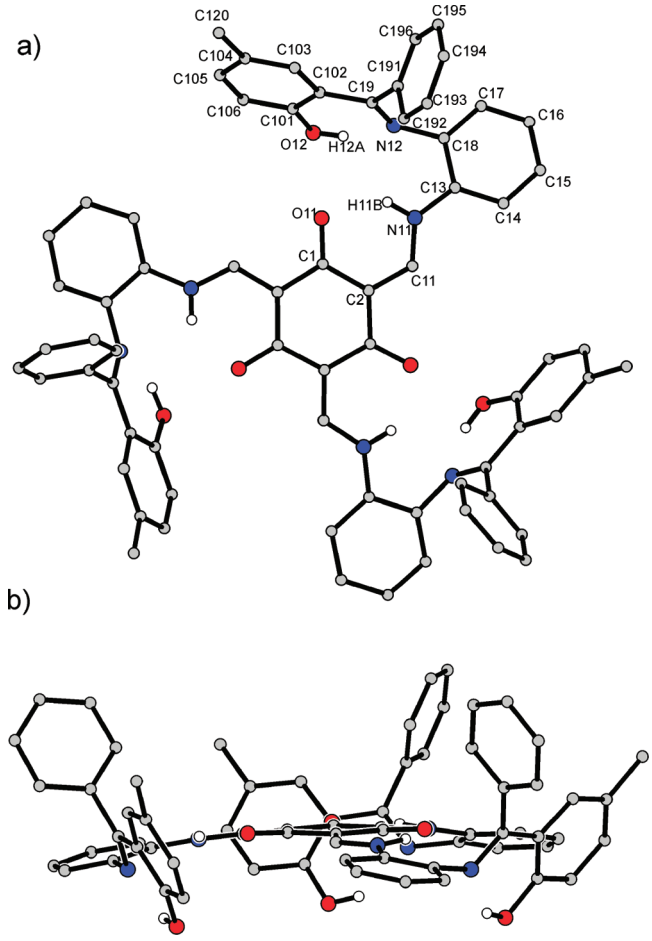

Figure 2. Molecular structure of H_6baron^{Me} in crystals of $H_6baron^{Me}{\cdot}C_5H_{12}$ with the numbering scheme used (a) drawn perpendicular to the central benzene ring of the phloroglucinol backbone and (b) drawn parallel to the central benzene ring of the phloroglucinol backbone. Hydrogen atoms are omitted for clarity with the exception of H11B and H12A.

around 30000 and 37000 cm^{-1} and a new very intensive low-energy feature at ~23000 cm^{-1}.

■ ANALYSIS AND DISCUSSION

Tautomerism and Resonance in Triplesalophen Ligands Analyzed in Solution by NMR and in the Solid State by Single-Crystal X-ray Diffraction. The triplesalen ligand system has been designed in order to enforce ferromagnetic couplings between three paramagnetic transition metal ions by the spin-polarization mechanism due to the *m*-phenylene arrangement.[11−21] Magnetic studies on Cu^{II}_3 and $(V^{IV}{=}O)_3$ triplesalen complexes[5−7] revealed that the exchange coupling is indeed ferromagnetic but only weakly, whereas the

Table 2. Comparison of Structural Parameters in Triplesalophen Ligands [Å]

	$C{-}O_{cent}$	$C{-}O_{term}$	$C{=}N_{cent}$	$C{=}N_{term}$	$C^{ar}{-}C^{imine}{}_{cent}$	$C^{ar}{-}C^{imine}{}_{term}$	$C^{ar}{-}C^{ar}{}_{cent}$	$C^{ar}{-}C^{ar}{}_{term}$
H_2carl^{Cl}	1.36	1.35	1.29	1.29	1.45	1.48	1.39	1.40
$H_6baron^{Me}{\cdot}C_5H_{12}$	1.25	1.35	1.32	1.29	1.38	1.47	1.46	1.39
$H_6baron^{Me}{\cdot}1.5CH_2Cl_2$	1.26	1.35	1.32	1.29	1.39	1.47	1.45	1.39
$H_6baron^{Cl}{\cdot}C_5H_{12}$	1.26	1.35	1.32	1.29	1.38	1.47	1.46	1.39
$H_6baron^{Br}{\cdot}C_5H_{12}$	1.25	1.35	1.32	1.29	1.38	1.47	1.46	1.39
H_6chand^{rac60}	1.27	1.36	1.31	1.28	1.43		1.45	
other heteroradialenes found in CSD[62−67]	1.26		1.33		1.38		1.45	

dx.doi.org/10.1021/jo202273s | J. Org. Chem. 2012, 77, 1435−1448

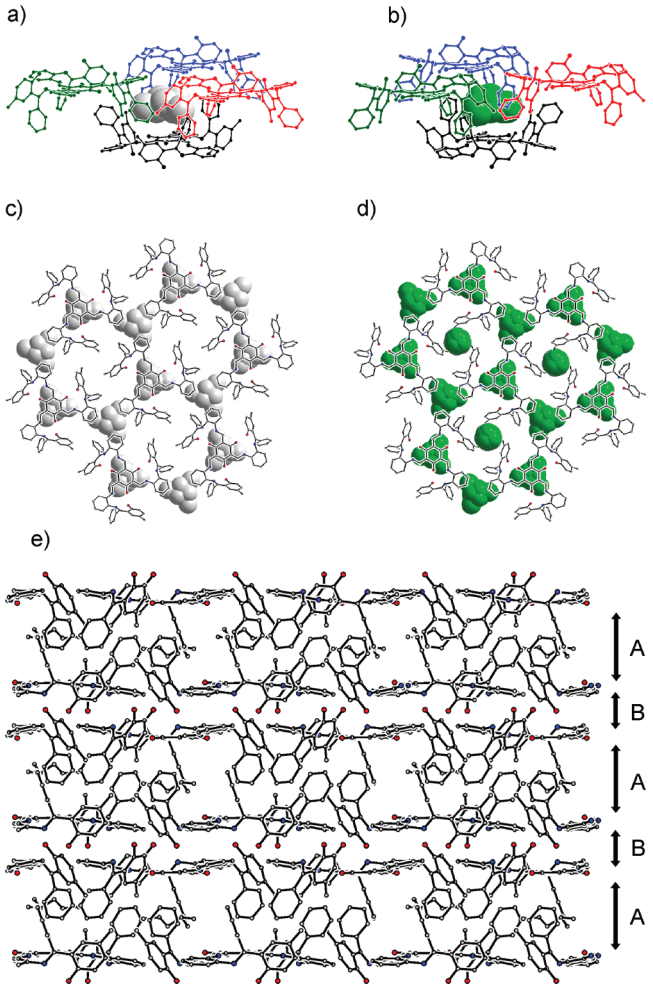

Figure 3. Illustration of the solvent encapsulation in (a) $H_6baron^{Me}{\cdot}C_5H_{12}$ and (b) $H_6baron^{Me}{\cdot}1.5CH_2Cl_2$. Part of the crystal structure of (c) $H_6baron^{Me}{\cdot}C_5H_{12}$ and (d) $H_6baron^{Me}{\cdot}1.5CH_2Cl_2$ showing the ligand in ball-and-stick representation and the solvent in the space-filling representation. (e) Illustration of the bilayer structure in crystals of $H_6baron^{Me}{\cdot}C_5H_{12}$ as a representative of all ligands showing the hydrophobic (A) and hydrophilic (B) compartments.

coupling is even slightly antiferromagnetic in Mn^{III}_3 complexes[59,68] and slightly antiferromagnetic to uncoupled in Fe^{III}_3 complexes.[60] This observation is contrary to the stronger ferromagnetic interactions observed in the related *N,N′,N″*-1,3,5-benzenetriyltris(oxamato) complexes.[69,70] Recently, we identified a possible reason for this unexpected magnetic behavior in our triplesalen complexes by NMR studies on the related phloroglucinol-based ligands H_3felden[9] and H_3felddien[10] (Scheme 4) based on the work of MacLachlan[62,71] and others on tris(*N*-salicylidenaniline)s.[63,65,67,72−76] These studies reveal that the central phloroglucinol backbone is not in the expected O-protonated tautomeric form but in the N-protonated tautomeric form (Scheme 5). Furthermore, this tautomer must be considered as a resonance hybrid of the neutral keto-enamine resonance structure **IV** with some contribution of the ionic phenolate-iminium resonance structure **III** (Scheme 5). The prevalence of the resonance structure **IV** in the ligands H_3felden[9] and H_3felddien[10] indicates the loss of the aromatic π system so that a π spin-polarization mechanism cannot be active. The combined analysis of solid-state molecular structures established by single-crystal X-ray

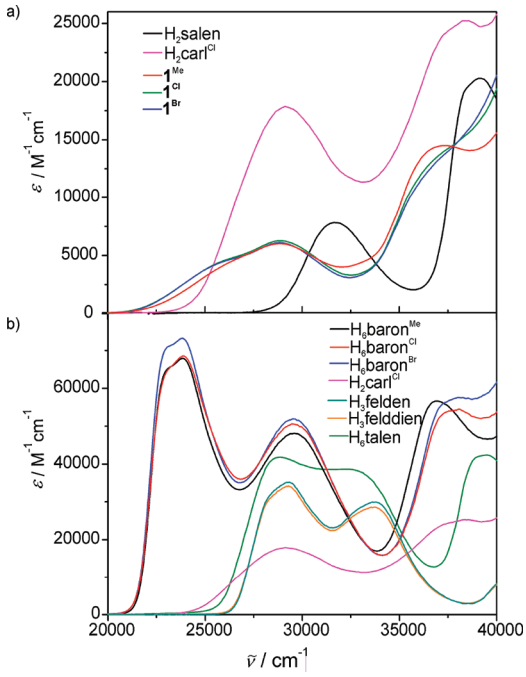

Figure 4. (a) Electronic absorption spectra of H_2salen, H_2carl^{Cl}, and the salophen half-units $\mathbf{1}^{R}$ (R = Me, Cl, Br), all measured in CH_2Cl_2. (b) Electronic absorption spectra of the ligands H_6baron^{R} (R = Me, Cl, Br), H_2carl^{Cl}, H_3felden, H_3felddien, and H_6talen, all measured in CH_2Cl_2. Note different *y*-scalings in the two figures.

diffraction and in solution by NMR spectroscopy of this series of triplesalophen ligands in combination with the unsymmetrical mononucleating salophen reference ligand H_2carl^{Cl} makes it possible to obtain more insight into this tautomerism-resonance senario.

The molecular structure of the mononucleating H_2carl^{Cl} reference exhibits no significant differences compared to known salophen ligands.[77,78] The C−O, C═N, and the mean benzene C^{ar}−C^{ar} bond lengths (Table 2) matches the values found in the literature (1.35, 1.29, and 1.40 Å, respectively).[77,78] The high-resolution single-crystal X-ray diffraction data for H_2carl^{Cl} allows the location of the acidic hydrogen atoms to be bound to the phenolic oxygen atoms O11 and O12 (Figure 1).

The ^{1}H NMR spectrum of H_2carl^{Cl} reveals two singlets at 14.12 ppm for O12*H* and at 12.94 ppm for O11*H* typical for salophen ligands.[78−80] The singlets at 8.38 ppm are also typical for imine groups.

Further evidence for the O-protonated tautomer in both compartments is provided by ^{13}C NMR spectroscopy. The ^{13}C NMR spectrum of H_2carl^{Cl} exhibits resonances at 161.3 ppm for C1 and at 161.4 ppm for C101 typical for salophen ligands (161 ppm)[80] and for enol-imines (160.9 ppm).[81] Claramunt et al. remarked that the ^{13}C resonance varies from ∼151 ppm for an enol-imine to ∼180 ppm for a pure keto-enamine tautomer,[82] making the ^{13}C resonance a powerful parameter to discern the relative tautomeric population. The ^{13}C NMR spectrum exhibits also resonances for the aldimine C11 (162.6 ppm) and the ketimine C19 (173.9 ppm) at typical chemical shifts.[79−81] Thus, X-ray diffraction and NMR spectroscopy demonstrate that in H_2carl^{Cl} the aldimine and ketimine moieties are in the enol-imine form in the solid state and in solution.

Contrarily, the analysis of the molecular structure of H_6baron^{R} (R = Me, Cl, Br) in crystals of $H_6baron^{R}{\cdot}C_5H_{12}$ and $H_6baron^{Me}{\cdot}1.5CH_2Cl_2$ reveal that the acidic protons of the

dx.doi.org/10.1021/jo202273s | J. Org. Chem. 2012, 77, 1435−1448

Scheme 4

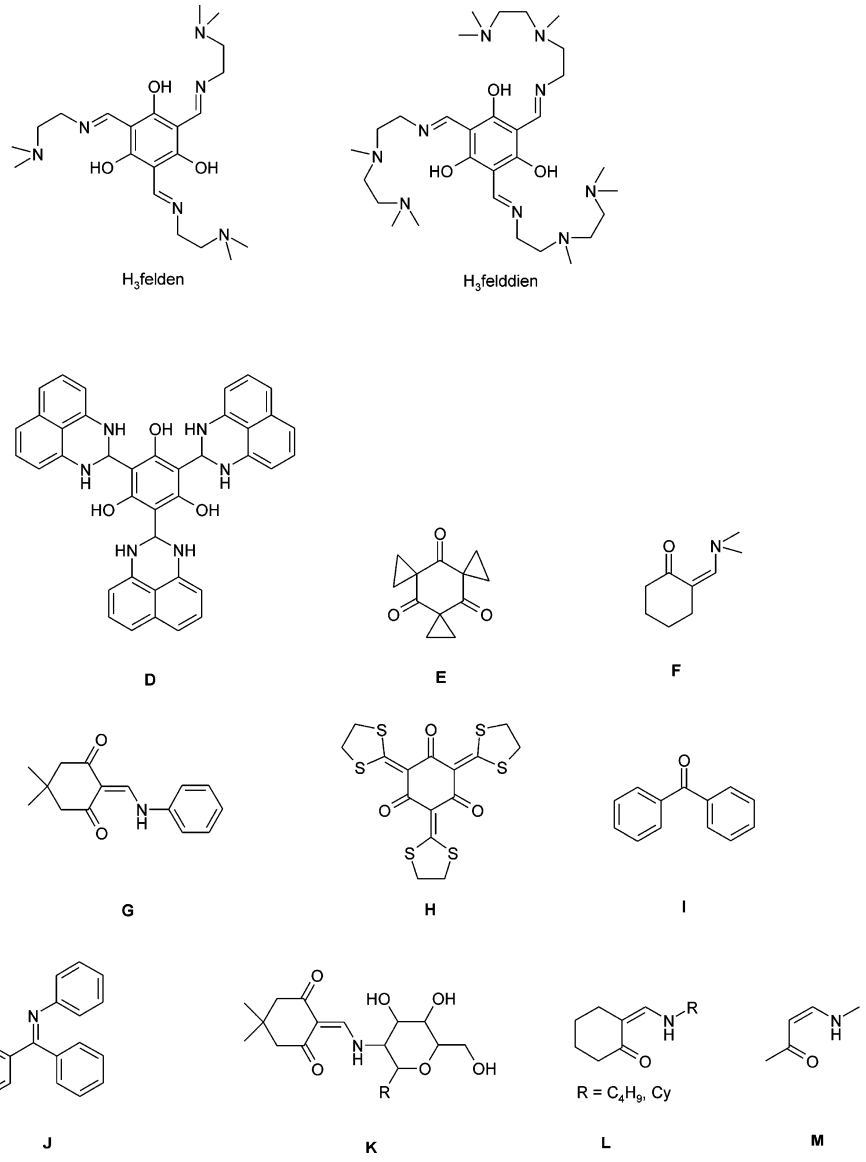

Scheme 5

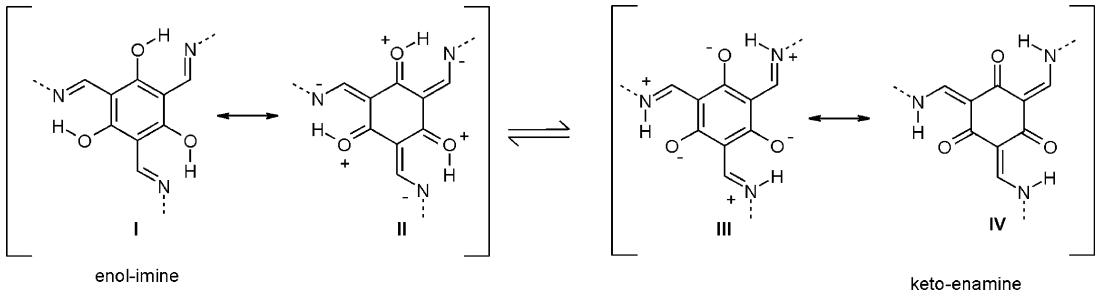

central aldimine moieties are not bond to O12 but bond to N11 (Figure 2). This different tautomerism scenario is corroborated by ^{1}H NMR spectroscopy. While the O12*H* resonance (13.85 ppm for R = Me; 14.02 ppm for R = Cl; 14.08 ppm for R = Br) is a singlet as in H_2carl^{Cl}, the N11*H* resonance is a doublet (J = 13 Hz; 13.49 ppm for R = Me, 13.52 ppm for R = Cl, and 13.54 ppm for R = Br). 2D ^{1}H,^{1}H COSY NMR experiments prove coupling with the "imine" proton C11*H*, which appears also as a doublet (J = 13 Hz; 8.65 ppm for R = Me; 8.54 ppm for R = Cl; 8.56 ppm for R = Br). This splitting pattern has already been observed for the N-protonated ligands $H_3felden$[9] and $H_3felddien$[10] as well as for tris(*N*-salicylideneaniline)s[62,71] and was proposed for the pure N-protonated tautomer.[83] These results demonstrate that the acidic protons are bond to O12 and N11 in solution as well.

dx.doi.org/10.1021/jo202273s | J. Org. Chem. 2012, 77, 1435–1448

Additionally, several structural and NMR spectroscopic features makes it possible to analyze the relative contributions of the resonance structures **III** and **IV** for the central phloroglucinol backbone. The C−O bond distances differ tremendously for the terminal C−O bonds (1.35 Å) and the central C−O bonds (1.25−1.26 Å). Comparison to H_2carl^{Cl} (1.35−1.36 Å) clearly establishes an usual enol-imine compartment for the terminal units. However, the central C−O bond length of 1.25−1.26 Å indicates severe double-bond character demonstrated by the comparison to the bond length of phenol **D** (1.39 Å)[84] and of triketone **E** (1.21 Å)[85] (Scheme 4).

The C^{ar}−C^{ar} bond lengths of the terminal phenols of 1.39 Å are in accord to those of H_2carl^{Cl} (1.39−1.40 Å) and are typical values for C^{ar}−C^{ar} bond distances in benzene rings (1.38 Å).[86] On the other hand, the central phloroglucinol unit has C^{ar}−C^{ar} bond distances of 1.45−1.46 Å, which also confirms a strong contribution of resonance structure **IV**. This is further confirmed by the short C^{ar}−C^{imine} central bond length of 1.38−1.39 Å, which indicates a strong double-bond character compared to those of the terminal compartment (1.47 Å) and that of H_2carl^{Cl} (1.48 Å). This effect is less strong in the bond length of the "imine" bond, which is only slightly longer for the central compartment (1.32 Å) as compared to the terminal compartment and H_2carl^{Cl} (1.29 Å).

It might be questioned that the elongation of the mean C^{ar}−C^{ar} bond length of the central compartment of H_6baron^{R} could be a result of the 6-fold substitution of the benzene ring. However, the 6-fold substituted phloroglucinol derivative **D** bearing saturated substituents in 2,4,6-positions (Scheme 4) exhibits a mean C−C bond length of 1.37 Å[84] typical for phenols (1.38 Å).[86] Also the sterically highly crowded substituents in 2,4,6-triacetyl-1,3,5-tris(dimethylthiocarbamoylthio)benzene[87] leading to a mean C^{ar}−C^{ar} bond length of 1.40 Å clearly demonstrate that six bulky substituents do not necessarily induce elongated bond lengths in the benzene ring.

This interpretation is corroborated by analysis of the ^{13}C resonances: the values of the terminal C101 (160.0 ppm for R = Me; 160.9 ppm for R = Cl; 161.4 ppm for R = Br) fit well with that of H_2carl^{Cl} (161.4 ppm), while the central C1 exhibits a chemical shift at lower field (185.2 ppm, 185.1 ppm, and 185.0 ppm for H_6baron^{Me}, H_6baron^{Cl}, and H_6baron^{Br}, respectively). Comparing these values to values of related compounds (157.6 ppm for **D**, 202.2 ppm for **E**, 197.1 ppm for **F**,[88] and 200.6 and 196.8 ppm for **G**[89]) strongly corroborates that the central compartment of H_6baron^{R} possess strong contributions of resonance structure **IV** (Scheme 5).

The terminal ketimine carbon atoms C19 exhibit ^{13}C chemical shifts (177.1 ppm for R = Me; 176.3 ppm for R = Cl; 176.2 ppm for R = Br) corresponding to that of H_2carl^{Cl} (176.3 ppm). Contrarily, the central aldimine ^{13}C resonance of C11 (148.2 ppm for R = Me; Cl, Br) are shifted to higher field relative to that of H_2carl^{Cl} (162.6 ppm). This shift is consistent with the formulation as keto-enamines (**F** 150.5 ppm[88] and **G** 151.0 ppm[89]). This assignment is also corroborated by the ^{13}C chemical shift of C2 (107.3 ppm for R = Me; Cl, Br) with is much closer to that of **F** (104.5 ppm) and **G** (110.1 ppm) than to that of H_2carl^{Cl} (119.4 ppm).

Some of these structural (Table 2) and NMR spectroscopic properties have been reported for tris(*N*-salicylidenaniline)s,[62−67,90] **H**,[91] H_6chand^{rac},[60] $H_3felden$,[9] and $H_3felddien$[10] and support the formulation of the central backbone of H_6baron^{R} to have a strong contribution of resonance structure **IV** (Scheme 5). This formulation comprised of a six-membered ring with six exocyclic C−C double bonds is reminiscent to [6]radialenes. Radialenes are cross-conjugated alicyclic hydrocarbons comprised of sp^2-hydridized ring carbon atoms and show as many exocyclic double bonds as possible.[92−95] Already in the first report on a radialene[96] and in a quantum-chemical study published shortly thereafter aiming to reproduce the electronic absorption spectrum,[97] it was concluded that [6]radialenes are not planar but should exhibit a deformed chair conformation of cyclohexane. This interpretation was later confirmed by several structural analyses of substituted [6]radialenes.[98−103] Based on structural and theoretical considerations, the cross-conjugated [6]radialenes are considered as nonaromatic alicycles.[92,93,97,104]

It must be noted that the structural properties of these [6]radialene exhibit significant differences to the triplesalophen ligands. Besides the planar central framework of the triplesalophen ligands as compared to the nonplanar framework of [6]radialenes mostly described as a chair conformation, the C−C distances in the ring of [6]radialenes are longer (1.49−1.50 vs 1.45−1.46 Å in H_6baron^{R}) and the exocyclic double-bonds are shorter (1.32−1.34 vs 1.38−1.39 Å in H_6baron^{R}) Additionally, the ^{13}C chemical shifts of the endocyclic carbon atoms are higher than that of the exocyclic ones (136.8 and 122.6 ppm, respectively) contrary to those of the triplesalophen ligands.[105]

These differences indicate that our ligands and other tris(*N*-salicylideneaniline)s cannot exclusively be formulated by resonance structure **IV** but also exhibit some contributions of **III** (Scheme 5). As a zwitterionic resonance structure **III** is energetically not accessible in [6]radialenes, the push−pull effect of the electron-withdrawing oxygen atoms and electron-donating nitrogen atoms stabilize this resonance structure **III** in our ligands. In this respect, compounds that are comprised of the structural motifs found in our ligands and in tris(*N*-salicylideneaniline)s[62−67] as well as in **H**[91] may be considered as heteroradialenes[93] in order to avoid misunderstandings with regards to structural and spectroscopic properties of [6]radialenes.

Recently, two [6]radialene derivatives have been reported, in which two neighboring exocyclic carbon atoms are connected either by a common sulfur or selenium bridge.[106] The molecular structures exhibit planar geometries and C−C bond distances of 1.45−1.46 Å in the ring and 1.36−1.37 Å for the exocyclic bonds. Thus, these two [6]radialenes with constraints induced by the five-membered rings deviate from the nonconstrained [6]radialenes as much as the triplesalophen ligands do. Interestingly, DFT calculations provide nucleus-independent chemical shifts (NICS) close to zero for the central ring. This is interpreted by the authors, that the ring can be considered to be practically nonaromatic. Furthermore, the authors compare the situation to that of benzene in a pure sigma state that does not include any contribution from π orbitals.[106]

Infrared Spectroscopy. Whereas the FTIR spectra of H_6baron^{R} (R = Me, Cl, Br) exhibit no significant bands for the OH and NH stretches in the 3100−2200 cm^{-1} region, 4 prominent bands between 1700 and 1400 cm^{-1} (Figure 5) are present, which do not correspond to the known salophen vibrations. In order to identify the IR signatures of the central heteroradialene backbone, the bands caused by the terminal ketimine compartments of H_6baron^{R} have to be identified.

Acetophenone exhibits a C═O stretch at 1692 cm^{-1}. Introduction of a *o*-hydroxy group results in a low-energy shift to 1648 cm^{-1}. The same trend is observed in benzophenone **I**, where the C═O stretch at 1664 cm^{-1} is shifted to 1624−1630 cm^{-1} in the respective 2-hydroxybenzophenones

dx.doi.org/10.1021/jo202273s | J. Org. Chem. 2012, 77, 1435−1448

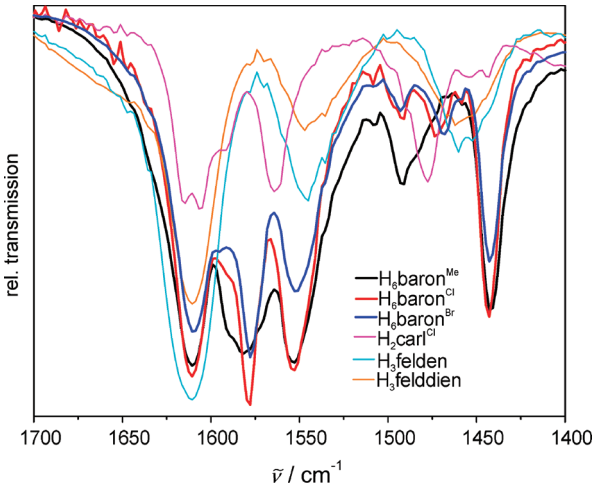

Figure 5. FTIR spectra of ligands H$_6$baron^R (R = Me, Cl, Br), H$_2$carl^{Cl}, H$_3$felden, and H$_3$felddien in the range of 1700−1400 cm^{-1}.

used as starting materials for **1**^{R}. The low-energy shift by introduction of an *o*-hydroxy group reflects the C=O bond order reduction induced by the hydrogen bond. This can be described by a zwitterionic protonated keto-enolate resonance structure in VB theory (Scheme 6).

Scheme 6

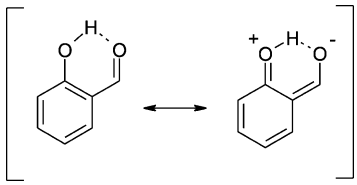

Formation of the phenylimine of benzophenone and **1**^{R} leads to a further low energy shift for the resulting C=N bond to 1616 cm^{-1} in imine **K**[107] and ∼1590 cm^{-1} in **1**^{R}. Thus the vibration at 1591 cm^{-1} in H$_2$carl^{Cl} and at ∼1580 cm^{-1} in H$_6$baron^R may be assigned to the terminal ketimine C=N stretch.

Benzaldehyde exhibits the C=O stretch at 1700 cm^{-1}, which shifts to 1665 cm^{-1} by incorporation of a *o*-hydroxy group in salicylaldehyde. Reaction with 1,2-phenylendiamine results in the formation of H$_2$salophen with a C=N stretch at 1616 cm^{-1}.[108−110] Thus, the band at 1614 cm^{-1} in H$_2$carl^{Cl} is assigned to the aldimine C=N stretch.

The bands at 1611 and 1553 cm^{-1} in the FTIR spectra of the triplesalophen ligands H$_6$baron^R are also present in FTIR spectra (Figure 5) of H$_3$felden (1611 and 1545 cm^{-1})[9] and H$_3$felddien (1611 and 1547 cm^{-1}).[10] The band at 1443 cm^{-1} is slightly shifted to lower frequencies compared to H$_3$felden (1460 cm^{-1}) and H$_3$felddien (1462 cm^{-1}). These three bands at 1611, 1533, and 1443 cm^{-1} might be characteristic for the heteroradialene structural motif. Interestingly, the salophen ligand H$_2$carl^{Cl} and the triplesalophen ligands H$_6$baron^R exhibit a vibration at about the same frequency (1614 and 1611 cm^{-1}, respectively) which is of different origin. This vibration is assigned to the aldimine of H$_2$carl^{Cl}, which is absent in H$_6$baron^R.

The comparison to the IR spectra of related molecules seems to be helpful. The IR spectrum of the α,β-unsaturated cyclohexanone **F** (Scheme 4) exhibits vibrations at 1650 and 1551 cm^{-1}, which have been assigned to the C=O and the C=C stretches, respectively.[111] The 1,3-diketones **G** and **L** with 2-enamine substituents have been reported to exhibit two different C=O stretches (1665 and 1600 cm^{-1} for **G**[112] and 1670 and 1605 cm^{-1} for **L**[113]). The vibration at higher energy was assigned to the C=O group not involved in hydrogen bonding and the low energy vibration to the C=O group involved in hydrogen bonding. Additionally, for **L** a band at 1585 cm^{-1} was assigned to a mixed ν(C=C)/δ(N−H) mode,[113] which appears in **G** at 1590 cm^{-1}.[112]

These comparisons indicate that the 1611 cm^{-1} mode in heteroradialenes has a strong C=O character and the 1552 cm^{-1} mode has a strong C=C character. It should be stressed that conflicting reports for assignment of the keto-enamines appeared in the literature. Dabrowski and Daboriwska performed intensive IR studies on simple keto-enamines **M**, conferring the nomenclature for vibrations of amides on vinylogene keto-enamines.[114] The energetically highest IR band at ∼1650 cm^{-1} was assigned to a vibrational mode comprised mainly of a C=O stretch ("amide-vinyloge-band I", **AVI**). The band at ∼1550 cm^{-1} (**AVII**) was assigned to a complicated normal mode, comprised of vibrations of the whole structure with pronounced N−H and C−N contributions. The third band at about 1455 cm^{-1} (**AVIII**) was assigned to a normal mode involving the whole system without providing specific assignments.

A different assignment was suggested later for the IR spectra of several isomers of keto-enamines like **N** based on DFT calculations.[115] The band at higher frequency was assigned to a vibrational mode mainly of C=C character rather than of C=O character. This assignment was supported by reports on the heteroradialene **H** for which the band at 1565 cm^{-1} was also assigned to the C=O stretch.[91]

In summary, the three bands at 1611, 1553, and 1443 cm^{-1} seem to be characteristic for the heteroradialene structural motif. Due to the conflicting reports we refrain from a definite assignment at the moment. We are currently performing a comprehensive DFT study to gain more insight into these vibrational modes.

Electronic Absorption Spectroscopy. The ligand H$_2$salen has a strong absorption at 31600 cm^{-1} with $\varepsilon \approx 7.9 \times 10^3$ M^{-1} cm^{-1} (Figure 4a),[2] which has been assigned to $\pi \rightarrow \pi^*$ transitions involving the imine group.[116−118] A higher energy band around 39100 cm^{-1} originates from $\pi \rightarrow \pi^*$ transitions associated with the phenolic chromophor.[116−118] The observed red shift and increased intensities of the imine $\pi \rightarrow \pi^*$ bands of H$_2$carl^{Cl} (29100 cm^{-1}, $\varepsilon \approx 17.9 \times 10^3$ M^{-1} cm^{-1}, Figure 4a) compared to H$_2$salen can be attributed to the larger π delocalization over the whole ligand caused by the substitution of the ethylene bridge in H$_2$salen by a phenylene bridge in H$_2$carl^{Cl}.[118]

By going from the mononucleating salophen ligand H$_2$carl^{Cl} to the trinucleating triplesalophen ligand H$_6$baron^R (Figure 4b), the $\pi \rightarrow \pi^*$ transition of H$_2$carl^{Cl} seems to split into two strong bands around 23000 and 30000 cm^{-1} with intensities of $\sim 7 \times 10^4$ and $\sim 5 \times 10^4$ M^{-1} cm^{-1}, respectively. A similar trend has been observed by going from the mononucleating salen ligand to the trinucleating triplesalen ligand (see H$_2$salen in Figure 4a and H$_6$talen in Figure 4b). As these strong absorptions in H$_6$talen also appear in H$_3$felden and H$_3$felddien (Figure 4b), they have been assigned to the heteroradialene backbone in these extended phloroglucinol ligands.[9,10]

Again, the extension of the π system from triplesalen to triplesalophen ligands shifts these strong absorptions from 28800 and 32400 cm^{-1} to 23000 and 30000 cm^{-1} with increased intensity

dx.doi.org/10.1021/jo202273s | J. Org. Chem. 2012, 77, 1435−1448

as has been observed by going from salen to salophen ligands. Absorption bands at similar energies with similar intensities are reported for other tris(*N*-salicylidenaniline) derivatives.[66]

The absorption features above 36000 cm^{-1} are present in all ligands that exhibit terminal enol-imine chromophores as well as in H_2salen, H_2carl^{Cl} and **1**^{R} but are absent in the spectra of H_3felddien and H_3felden consistent with the assignment of these transitions to the terminal enol-imine chromophores.

CONCLUSIONS

1. The triplesalophen ligand system has been synthesized in a convergent approach by reaction the trialdehyde of phloroglucinol with salophen ketimine half-units in contrast to the divergent approach of the triplesalen ligand system by reaction of the triplesalen ketimine half-unit with aldehydes.
2. The use of the complementary methods X-ray diffraction, NMR, IR, and UV−vis spectroscopies affords signatures of the central heteroradialene in extended phloroglucinol ligands not only for NMR spectroscopies but also for structural parameters and IR and UV−vis spectroscopies:
   NMR: doublet for enamine proton at ∼13.5 ppm; doublet for "imine" proton at ∼8.6 ppm; ^{13}C C═O at ∼185 ppm compared to ∼161 ppm for *C*−O in enol-imines; ^{13}C "imine" at ∼148 ppm compared to ∼162 ppm in enol-imines.
   RSA: d(C═O) ∼1.25−1.26 Å compared to 1.39 Å in phenol **D**; d(C^{ar}−C^{imine}) ∼1.38−1.39 Å compared to 1.47 Å in H_2carl^{Cl}; d(C^{ar}−C^{ar}) ∼1.45−1.46 Å compared to 1.38 Å in benzene.
   IR: three intense bands at 1611, 1553, and 1443 cm^{-1} with the band at 1443 cm^{-1} differing slightly to 1460 cm^{-1} in H_3felden and 1462 cm^{-1} in H_3felddien.
   UV−vis: intense bands at 23000 cm^{-1} (ε = ∼7 × 10^4 M^{-1} cm^{-1}) and 30000 cm^{-1} (ε = ∼5 × 10^4 M^{-1} cm^{-1}) that are even more intense and red-shifted compared to the triplesalen ligand system at 29000 cm^{-1} (ε = ∼4.2 × 10^4 M^{-1} cm^{-1}) and 34000 cm^{-1} (ε = ∼3.9 × 10^4 M^{-1} cm^{-1}) demonstrating the participation of the phenylenediamine backbone in the delocalized π system.
3. Extended phloroglucinol ligands are in the N-protonated tautomeric form, in which the keto-enamine resonance structure **IV** has strong contributions. However, in these heteroradialenes are also some contributions of the ionic resonance structure **III** in contrast to [6]radialenes.

EXPERIMENTAL SECTION

Preparations of Compounds. Solvents and starting materials were of the highest commercially available purity and used as received except for ethanol and tetrahydrofuran, which were dried over CaH_2 and distilled under an argon atmosphere before use. All reactions were performed using standard Schlenk-conditions except for the synthesis of H_2carl^{Cl}. 2,4,6-Triformylphloroglucinol (**2**) was synthesized by a literature procedure.[62] The synthesis of **1**^{Cl} and H_2carl^{Cl} were performed by using modified literature procedures.[61] H_6baron^{Br} has been communicated recently.[46] The assignments of the NMR resonances in all products were supported by 2D COSY, HMBC, and HMQC spectroscopy and the numbering was done according to the numbering scheme in Figures 1 and 2.

2-[(2-Aminophenylimino)phenylmethyl]-4-methylphenol (1^{Me}). 5-Methyl-2-hydroxybenzophenone (3.00 g, 14.13 mmol) and 1,2-phenylenediamine (1.56, 14.43 mmol, 1.02 equiv) were suspended in ethanol (10 mL). This suspension was stirred at 40 °C until an orange solution has formed. Piperidine (1.50 mL, 15.18 mmol, 1.07 equiv) and triethylorthoformate (3.00 mL, 18.06 mmol, 1.28 equiv) were added. The reaction mixture was heated at reflux for 3 h. While cooling to room temperature orange needles were formed. The precipitate was collected by filtration, washed with ethanol (20 mL), and dried in vacuum. Yield: 1.98 g (46%). Mp 195−197 °C. ^{1}H NMR (500.05 MHz, $CDCl_3$) δ 14.20 (s, 1H; O12*H*), 7.35 (m, 3H; C193−C195*H*), 7.21 (m, 3H; C105*H*, C192*H*, C196*H*), 7.01 (d, 1H; C106*H*), 6.89 (d, 1H; C103*H*), 6.84 (dt, 1H; C15*H*), 6.69 (dd, 1H; C14*H*), 6.42 (dt, 1H; C16*H*), 6.28 (dd, 1H; C17*H*), 3.85 (s, 2H; N11H_2), 2.18 (s, 3H; C120H_3). ^{13}C NMR (125.75 MHz, $CDCl_3$) δ 175.1 (C19), 160.1 (C101), 139.2 (C13), 134.3 (C191), 134.2 (C105), 134.0 (C18), 132.1 (C103), 129.1 (C194), 128.3 (C192, C196), 128.1 (C193, C195), 127.1 (C104), 125.6 (C15), 121.8 (C17), 119.6 (C102), 117.9 (C16), 117.6 (C106), 115.1 (C14), 20.5 (C120). IR (KBr) ν 3458 m, 3366s, 1626 m, 1597s, 1562 m, 1493 m, 1400w, 1335 m, 1292 m, 1240 m, 1132 m, 827 m, 746s, 712 m cm^{-1}. ESI-MS ($CHCl_3$/MeOH) m/z 303.1 [M + H]$^+$, 325.0 [M + Na]$^+$, 626.7 [2M + Na]$^+$, 927.5 [3M + Na]$^+$. Anal. Calcd for $C_{20}H_{18}N_2O$: C, 79.44; H, 6.00; N, 9.26. Found: C, 79.32; H, 6.00; N, 9.09.

2-[(2-Aminophenylimino)phenylmethyl]-4-chlorophenol (1^{Cl}). 5-Chloro-2-hydroxybenzophenone (2.00 g, 8.60 mmol) and 1,2-phenylenediamine (0.96 g, 8.88 mmol, 1.03 equiv) were suspended in ethanol (7.5 mL). This suspension was stirred at 40 °C until an orange solution has formed. Piperidine (0.90 mL, 9.10 mmol, 1.06 equiv) and triethylorthoformate (1.70 mL, 10.23 mmol, 1.20 equiv) were added. The reaction mixture was heated at reflux for 3 h. While cooling to room temperature orange needles were formed. The precipitate was collected by filtration, washed with ethanol (10 mL), and dried in vacuum. Yield: 1.69 g (61%). Mp 194−196 °C [lit.[61] 192 °C]. ^{1}H NMR (500.05 MHz, $CDCl_3$) δ 14.46 (s, 1H; O12*H*), 7.36 (m, 3H; C193*H*-C195*H*), 7.32 (dd, 1H; C105*H*), 7.19 (dd, 2H; C192*H*, C196*H*), 7.07 (d, 1H; C103*H*), 7.03 (d, 1H; C106*H*), 6.85 (dt, 1H; C15*H*), 6.69 (dd, 1H; C14*H*), 6.42 (dt, 1H; C16*H*), 6.26 (dd, 1H; C17*H*), 3.84 (s, 2H; N11H_2). ^{13}C NMR (125.75 MHz, $CDCl_3$) δ 174.1 (C19), 161.0 (C101), 139.3 (C13), 133.5 (C191), 133.4 (C18), 133.1 (C105), 131.2 (C103), 129.5 (C194), 128.2 (C192, C196), 128.4 (C193, C195), 126.1 (C15), 122.8 (C104), 121.8 (C17), 120.9 (C102), 119.5 (C106), 118.0 (C16), 115.3 (C14). IR (KBr) ν 3458 m, 3368s, 1622 m, 1591s, 1557 m, 1489 m, 1392w, 1329 m, 1281 m, 1236 m, 1134 m, 927 m, 829 m, 743s, 704 m cm^{-1}. ESI-MS ($CHCl_3$/MeOH) m/z 323.1 [M + H]$^+$, 345.1 [M + Na]$^+$, 666.3 [2M + Na]$^+$. Anal. Calcd for $C_{19}H_{15}N_2OCl$: C, 70.70; H, 4.68; N, 8.68. Found: C, 70.67; H, 4.79; N, 8.64.

2-[(2-Aminophenylimino)phenylmethyl]-4-bromophenol (1^{Br}). 5-Bromo-2-hydroxybenzophenone (2.77 g, 10.00 mmol) and 1,2-phenylenediamine (1.15 g, 10.00 mmol, 1.00 equiv) were suspended in ethanol (6.0 mL). The suspension was stirred at 40 °C until an orange solution has formed. Piperidine (1.00 mL, 10.00 mmol, 1.00 equiv) and triethylorthoformate (2.00 mL, 12.40 mol, 1.20 equiv) were added. The reaction mixture was heated at reflux for 3 h. While cooling to room temperature orange needles were formed. The precipitate was collected by filtration, washed with ethanol (8 mL), and dried in vacuum. Yield: 2.28 g (62%). Mp 191−192 °C. ^{1}H NMR (500.05 MHz, $CDCl_3$) δ 14.48 (s, 1H; O12*H*), 7.45 (dd, 1H; C105*H*), 7.37 (m, 3H; C193*H*-C195*H*), 7.20 (d, 1H; C103*H*), 7.18 (m, 2H; C192*H*, C196*H*), 6.97 (d, 1H; C106*H*), 6.85 (dt, 1H; C15*H*), 6.70 (dt, 1H; C14*H*), 6.42 (dt, 1H; C16*H*), 6.26 (dd, 1H; C17*H*), 3.88 (s, 2H; N11H_2). ^{13}C NMR (125.75 MHz, $CDCl_3$) δ 174.2 (C19), 161.6 (C101), 139.3 (C13), 136.1 (C105), 134.3 (C103), 133.6 (C191), 133.5 (C18), 129.7 (C194), 128.6 (C193, C195), 128.4 (C192, C196), 126.3 (C15), 122.0 (C17), 121.6 (C102); 120.1 (C106), 118.3 (C16), 115.5 (C14), 109.9 (C104). IR (KBr) ν 3458 m, 3368s, 1624 m, 1589s, 1555 m, 1491 m, 1478 m, 1385w, 1329 m, 1287 m, 1238 m, 1134 m, 970 m, 827 m, 743s, 702 m cm^{-1}. ESI-MS ($CHCl_3$/MeOH) m/z 369.0 [M + H]$^+$, 389.0 [M + Na]$^+$. Anal.

Table 3. Crystallographic Data for $H_6baron^{R}\cdot C_5H_{12}$, $H_6baron^{Me}\cdot 1.5CH_2Cl_2$, and H_2carl^{Cl}

	compound				
	$H_6baron^{Me}\cdot C_5H_{12}$	$H_6baron^{Me}\cdot 1.5CH_2Cl_2$	$H_6baron^{Cl}\cdot C_5H_{12}$	$H_6baron^{Br}\cdot C_5H_{12}$	H_2carl^{Cl}
chem formula	$C_{69}H_{54}N_6O_6\cdot C_5H_{12}$	$C_{69}H_{54}N_6O_6\cdot 1.5CH_2Cl_2$	$C_{66}H_{45}N_6O_5Cl_3\cdot C_5H_{12}$	$C_{66}H_{45}N_6O_5Br_3\cdot C_5H_{12}$	$C_{26}H_{19}N_2O_2$
fw (g mol^{-1})	1135.33	1190.57	1196.58	1329.96	426.88
T (K)	173(2)	100(2)	173(2)	173(2)	100(2)
space group	$P\bar{3}$	$P\bar{3}$	$P\bar{3}$	$P\bar{3}$	$P\bar{1}$
a (Å)	17.9054(8)	17.6734(6)	17.9406(6)	18.0254(6)	8.8280(2)
b (Å)	17.9054(8)	17.6734(6)	17.9406(6)	18.0254(6)	9.8280(2)
c (Å)	11.0374(7)	11.0022(4)	10.8992(5)	11.0413(5)	12.6380(3)
α (deg)	90.00	90.00	90.00	90.00	87.0450(12)
β (deg)	90.00	90.00	90.00	90.00	70.9630(13)
γ (deg)	120.00	120.00	120.00	120.00	87.2910(14)
V (Å^3)	3064.5(3)	2976.12(18)	3038.1(2)	3106.9(2)	2383.6(3)
Z	2	2	2	2	2
ρ_{calc} (g cm^{-3})	1.230	1.329	1.308	1.422	1.370
λ (Å); μ (Mo Kα, mm^{-1})	0.71073, 0.079	0.71073; 0.215	0.71073; 0.211	0.71073; 2.006	0.71073; 0.211
crystal size (mm)	0.40 × 0.26 × 0.14	0.20 × 0.15 × 0.03	0.46 × 0.40 × 0.20	0.34 × 0.30 × 0.12	0.32 × 0.30 × 0.28
coll reflns; $2\theta_{max}$	15295; 24.99	20868; 24.99	16462; 26.00	18384; 26.97	7073; 25.00
unique reflns	3556 (R_{int} = 0.0277)	3483 (R_{int} = 0.0301)	3967 (R_{int} = 0.0253)	4465 (R_{int} = 0.0257)	3626 (R_{int} = 0.0139)
obs reflns ($I > 2\sigma(I)$)	2697	2552	3196	3570	3424
data/restraints/parameters	3556/3/257	3483/0/311	3967/3/256	4465/2/256	288
goodness-of-fit[a] on F^2	1.024	1.026	0.969	1.026	1.017
$R1$[b]; $wR2$[c] ($I > 2\sigma(I)$)	0.0557; 0.1572	0.0424; 0.0986	0.0532; 0.1456	0.0365; 0.0912	0.0302; 0.0788
max/min residuals (e Å^{-3})	0.989 and −0.204	0.277 and −0.300	0.850 and −0.255	0.667 and −0.380	0.208 and −0.227

[a] GooF = $[\sum w(F_o^2 - F_c^2)^2]/(n-p)]^{1/2}$ [b] $R1 = \sum||F_o| - |F_c||/\sum|F_o|$ [c] $wR2 = [\sum[w(F_o^2 - F_c^2)^2]/\sum[w(F_o^2)^2]]^{1/2}$, in which $w = 1/[\sigma^2(F_o^2) + (aP)^2 + bP]$, $P = (F_o^2 + 2F_c^2)/3$

Calcd for $C_{19}H_{15}N_2OBr$: C, 62.14; H, 4.12; N, 7.63. Found: C, 62.14; H, 4.29; N, 7.49.

***N*-Phenyl-*N*-(2-hydroxy-5-chlorophenyl)-*N*′-(2-hydroxyphenyl)-1,2-phenylenediamine (H_2carl^{Cl}).** To a hot suspension of $\mathbf{1}^{Cl}$ (1.05 g, 3.25 mmol) in methanol (10 mL) were added salicylaldehyde (0.35 mL, 3.35 mmol, 1.03 equiv) and piperidine (0.5 mL, 5.06 mmol, 1.56 equiv). The resulting yellow suspension was heated at reflux for 0.5 h. After cooling to room temperature, the yellow precipitate was collected by filtration, washed with methanol (20 mL), and recrystallized from toluene/pentane. Yield: 0.86 g (60%). Mp 213−214 °C. ^{1}H NMR (600.13 MHz, $CDCl_3$) δ 14.12 (s, 1H; O12*H*), 12.94 (s, 1H; O11*H*), 8.38 (s, 1H; C11*H*), 7.37 (dt, 1H; C5*H*), 7.32 (m, 2H; C3*H*, C105*H*), 7.29 (m, 1H; C194*H*), 7.22 (t, 2H; C193*H*, C195*H*), 7.07 (m, 6H; C14*H*-C16*H*, C106*H*, C192*H*, C196*H*), 7.03 (d, 1H; C103*H*), 6.98 (d, 1H; C6*H*), 6.92 (t, 1H; C4*H*), 6.80 (m, 1H; C17*H*). ^{13}C NMR (125.75 MHz, $CDCl_3$) δ 173.9 (C19), 162.6 (C11), 161.4 (C101), 161.3 (C1), 141.6 (C18), 139.7 (C13), 133.9 (C191), 133.4 (C5), 132.3 (C3), 131.4 (C103), 129.4 (C194), 128.4 (C192, C196), 128.2 (C193, C195), 127.1 (C16), 126.0 (C15), 123.1 (C17), 122.7 (C104), 119.8 (C106), 119.4 (C2), 119.1 (C6), 118.5 (C14), 117.6 (C4). IR (KBr) ν 1614s, 1607s, 1564s, 1477 m, 1331 m, 1284 m, 1238 m, 758 m, 702 m cm^{-1}. ESI-MS ($CHCl_3$/MeOH) m/z 427.2 $[M + H]^+$, 449.2 $[M + Na]^+$, 874.6 $[2M + Na]^+$. Anal. Calcd for $C_{26}H_{19}N_2O_2Cl$: C, 73.15; H, 4.49; N, 6.56. Found: C, 73.29; H, 4.38; N, 6.59.

2,4,6-Tris{[2-((5-methyl-2-hydroxyphenyl)phenylmethylimino)-phenylimino]-methyl}-1,3,5-trihydroxybenzene (H_6baron^{Me}). Compounds **2** (0.21 g, 1.00 mmol) and $\mathbf{1}^{Me}$ (1.81 g, 5.99 mmol, 5.99 equiv) were dissolved in tetrahydrofuran (60 mL). The resulting orange solution was stirred at room temperature for 3 d, during which a yellow precipitate formed. It was collected by filtration, washed with methanol (30 mL), and dried in vacuum. H_6baron^{Me} was isolated as a bright yellow solid. Yield: 0.98 g (93%). Mp 246−248 °C (decomp). ^{1}H NMR (500.25 MHz; $C_2D_2Cl_4$) δ 13.85 (s, 3H; O12*H*), 13.49 (d, 3H; ^3J = 13 Hz, N11*H*), 8.65 (d, 3H; ^3J = 13 Hz, C11*H*), 7.32 (m, 15H; C14*H*, C105*H*, C193*H*-C195*H*), 7.15 (d, 3H; C106*H*), 7.12 (dd, 6H; C192*H*, C196*H*), 7.05 (dd, 3H; C15*H*), 6.99 (d, 3H; C103*H*), 6.87 (dd, 3H; C16*H*), 6.50 (d, 3H; C17*H*), 2.23 (s, 9H; C120H_3). ^{13}C NMR (125.75 MHz, $C_2D_2Cl_4$) δ 185.2 (C1), 177.1 (C19), 160.0 (C101), 148.2 (C11), 138.1 (C18), 134.8 (C105), 133.7 (C191), 132.7 (C103), 131.5 (C13), 129.2 (C194), 129.3 (C193, C195), 128.3 (C192, C196), 127.5 (C104), 125.5 (C15), 125.0 (C16), 122.9 (C17), 119.4 (C102), 117.8 (C106), 115.1 (C14), 107.3 (C2). IR (KBr) ν 1611s, 1582s, 1553s, 1443 m, 1294 m, 1263 m, 1234 m, 750w, 704w cm^{-1}. MALDI-TOF-MS (DHB) m/z: 1063.5 $[M + H]^+$, 1085.5 $[M + Na]^+$. Anal. Calcd for $C_{69}H_{54}N_6O_6$ (H_6baron^{Me}): C, 77.95; H, 5.12; N, 7.90. Found: C, 77.91; H, 5.45; N, 7.70.

2,4,6-Tris{[2-((5-chloro-2-hydroxyphenyl)phenylmethylimino)-phenylimino]-methyl}-1,3,5-trihydroxybenzene (H_6baron^{Cl}). Compounds **2** (0.065 g, 0.31 mmol) and $\mathbf{1}^{Cl}$ (0.58 g, 1.81 mmol, 6.00 equiv) were dissolved in tetrahydrofuran (18 mL). The resulting orange solution was stirred at room temperature for 3 d, during which a yellow precipitate was formed. It was collected by filtration, washed with methanol (10 mL), and dried in vacuum. H_6baron^{Cl} was isolated as a bright yellow solid. Yield: 0.34 g (98%). Mp 243−245 °C (decomp). ^{1}H NMR (600.13 MHz; $C_2D_2Cl_4$) δ 14.02 (s, 3H; O12*H*), 13.52 (d, 3H; ^3J = 13 Hz, N11*H*), 8.54 (d, 3H; ^3J = 13 Hz, C11*H*), 7.43 (dd, 3H; C105*H*), 7.32 (m, 9H; C193*H*-C195*H*), 7.17 (d, 3H; C106*H*), 7.14 (m, 9H; C14*H*), 6.98 (m, 3H; C15*H*), 6.87 (t, 3H; C16*H*), 6.56 (d, 3H; C17*H*). ^{13}C NMR (125.75 MHz, $C_2D_2Cl_4$) δ 185.1 (C1), 176.3 (C19), 160.9 (C101), 148.2 (C11), 137.5 (C18), 133.6 (C105), 132.9 (C191), 131.6 (C103), 131.1 (C13), 129.7 (C194), 128.4 (C193, C195), 128.0 (C192, C196), 125.9 (C15), 125.0 (C16), 122.8 (C17), 122.7 (C104), 120.6 (C102), 119.5 (C106), 115.1 (C14), 107.3 (C2). IR (KBr) ν 1611s, 1578s, 1553s, 1443 m, 1294 m, 1265 m, 1234 m, 700w cm^{-1}. MALDI-TOF-MS (DHB) m/z: 1124.9 $[M + H]^+$, 1146.9 $[M + Na]^+$. Anal. Calcd for $C_{70}H_{54}Cl_3N_6O_{7.5}$ ($H_6baron^{Cl}\cdot THF\cdot 0.5H_2O$): C, 69.74; H, 4.52; N, 6.97. Found: C, 69.75; H, 4.38; N, 7.03.

2,4,6-Tris{[2-((5-bromo-2-hydroxyphenyl)phenylmethylimino)-phenylimino]-methyl}-1,3,5-trihydroxybenzene (H_6baron^{Br}). Compounds **2** (0.10 g, 0.48 mmol) and $\mathbf{1}^{Br}$ (1.01 g, 2.78 mmol, 5.8 equiv) were dissolved in tetrahydrofuran (30 mL). The resulting orange solution was stirred at room temperature for 3 d, during which a yellow precipitate was formed. It was collected by filtration, washed with methanol (10 mL), and dried in vacuum.

dx.doi.org/10.1021/jo202273s | J. Org. Chem. 2012, 77, 1435−1448

H_6baron^{Br} was isolated as a bright yellow solid. Yield: 0.58 g (92%). Mp 235−238 °C (decomp). ^{1}H NMR (500.25 MHz; $C_2D_2Cl_4$) δ 14.08 (s, 3H; O12*H*), 13.54 (d, 3H; ^3J = 13 Hz N11*H*), 8.56 (d, 3H; ^3J = 13 Hz, C11*H*), 7.58 (dd, 3H; C105*H*), 7.33 (m, 9H; C193*H*-C195*H*), 7.28 (d, 3H; C103*H*), 7.23 (d, 3H; C14*H*), 7.06 (dd, 3H; C15*H*), 6.89 (dd, 3H; C16*H*), 6.55 (d, 3H; C17*H*). ^{13}C NMR (125.75 MHz, $C_2D_2Cl_4$) δ 185.0 (C1), 176.2 (C19), 161.4 (C101), 148.2 (C11), 137.4 (C18), 136.3 (C105), 134.6 (C103), 132.8 (C191), 131.2 (C13), 129.7 (C194), 128.4 (C193, C195), 128.0 (C192, C196), 126.0 (C15), 125.0 (C16), 122.7 (C17), 121.3 (C102), 120.0 (C106), 115.1 (C14), 109.9 (C104), 107.3 (C2). IR (KBr) ν 1611s, 1578s, 1553s, 1493w, 1443 m, 1331w, 1290 m, 1265 m, 1234 m, 750w cm^{-1}. MALDI-TOF-MS (DHB) *m*/*z*: 1258.5 $[M]^+$, 1281.5 $[M + Na]^+$, 1298.0 $[M + K]^+$. Anal. Calcd for $C_{72}H_{57}N_6O_{7.5}Br_3$ (H_6baron^{Br}·1.5THF): C, 63.31; H, 4.21; N, 6.15. Found: C, 63.65; H, 4.34; N, 6.36.

X-ray Crystallography. Yellow single crystals of H_6baron^{R}·C_5H_{12} (R = Me, Cl, Br) and H_6baron^{Me}·1.5CH_2Cl_2 and red single crystals of H_2carl^{Cl} were removed from the mother liquor, coated with oil, and immediately cooled to 183(2) K (100(2) K for H_2carl^{Cl} and H_6baron^{Me}·1.5CH_2Cl_2) on a diffractometer (sealed tube, Mo Kα radiation (λ = 0.71073 Å), graphite monochromator). An empirical absorption correction using equivalent reflections was performed with the program SADABS 2.10 (2008/1 for H_6baron^{Me}·1.5CH_2Cl_2).[119] The structures were solved with the program SHELXS-97[120] and refined using SHELXL-97.[120] The crystal lattice of H_6baron^{R}·C_5H_{12} contains one pentane molecule per formula unit, which is disordered around a 3-fold crystallographic axis. No hydrogen atoms could be localized at the pentane molecules. The crystal lattice of H_6baron^{Me}·1.5CH_2Cl_2 contains one disordered dichloromethane molecule on a crystallographic 3 axis and one disordered dichloromethane molecule on a crystallographic $\bar{3}$ axis. The carbon atom of the latter and all hydrogen atoms of the dichloromethane molecules could not be localized. All other hydrogen atoms were refined in calculated positions except the N−H and O−H hydrogen atoms for H_2carl^{Cl} and H_6baron^{Me}·1.5CH_2Cl_2, which could be localized from a difference Fourier map and refined without restraints. Crystal data and further details concerning the crystal structure determination are found in Table 3.

Other Physical Measurements. Infrared spectra (400−4000 cm^{-1}) of solid samples were recorded on a FTIR spectrometer as KBr disks. UV−vis−NIR absorption spectra of solutions were measured in the range 200−1200 nm at ambient temperatures. ^{1}H and ^{13}C NMR spectra were measured on a 500 MHz or a 600 MHz spectrometer using the solvent as an internal standard.

■ ASSOCIATED CONTENT

Supporting Information

^{1}H and ^{13}C NMR spectra of H_6baron^{R} (R = Me, Cl, Br). Thermal ellipsoid plots and crystallographic data (CIF format) of the ligands. This material is available free of charge via the Internet at http://pubs.acs.org.

■ AUTHOR INFORMATION

Corresponding Author

*E-mail: thorsten.glaser@uni-bielefeld.de.

■ ACKNOWLEDGMENTS

This work was supported by the DFG (FOR945 "Nanomagnets: from Synthesis *via* Interactions with Surfaces to Function"), the Fonds der Chemischen Industrie, and Bielefeld University.

■ REFERENCES

(1) Glaser, T.; Heidemeier, M.; Lügger, T. *Dalton Trans.* **2003**, 2381−2383.
(2) Glaser, T.; Heidemeier, M.; Fröhlich, R.; Hildebrandt, P.; Bothe, E.; Bill, E. *Inorg. Chem.* **2005**, *44*, 5467−5482.
(3) Glaser, T. *Chem. Commun.* **2011**, *47*, 116−130.
(4) Glaser, T.; Gerenkamp, M.; Fröhlich, R. *Angew. Chem., Int. Ed.* **2002**, *41*, 3823−3825.
(5) Glaser, T.; Heidemeier, M.; Grimme, S.; Bill, E. *Inorg. Chem.* **2004**, *43*, 5192−5194.
(6) Glaser, T.; Heidemeier, M.; Strautmann, J. B. H.; Bögge, H.; Stammler, A.; Krickemeyer, E.; Huenerbein, R.; Grimme, S.; Bothe, E.; Bill, E. *Chem.—Eur. J.* **2007**, *13*, 9191−9206.
(7) Theil, H.; Frhr, v.; Richthofen, C.-G.; Stammler, A.; Bögge, H.; Glaser, T. *Inorg. Chim. Acta* **2008**, *361*, 916−924.
(8) Walleck, S.; Theil, H.; Heidemeier, M.; Heinze-Brückner, G.; Stammler, A.; Bögge, H.; Glaser, T. *Inorg. Chim. Acta* **2010**, *363*, 4287−4294.
(9) Feldscher, B.; Stammler, A.; Bögge, H.; Glaser, T. *Dalton Trans.* **2010**, *39*, 11675−11685.
(10) Feldscher, B.; Stammler, A.; Bögge, H.; Glaser, T. *Polyhedron* **2011**, *30*, 3038−3047.
(11) McConnell, H. M. *J. Chem. Phys.* **1963**, *39*, 1910.
(12) Longuet-Higgins, H. C. *J. Chem. Phys.* **1950**, *18*, 265−274.
(13) Iwamura, H. *Adv. Phys. Org. Chem.* **1990**, *26*, 179−253.
(14) Cano, J.; Ruiz, E.; Alvarez, S.; Verdaguer, M. *Comments Inorg. Chem.* **1998**, *20*, 27−56.
(15) Dougherty, D. A. *Acc. Chem. Res.* **1991**, *24*, 88−94.
(16) Karafiloglou, P. *J. Chem. Phys.* **1985**, *82*, 3728−3740.
(17) Ovchinnikov, A. A. *Theor. Chim. Acta* **1978**, *47*, 297−304.
(18) Glaser, T.; Lügger, T.; Fröhlich, R. *Eur. J. Inorg. Chem.* **2004**, 394−400.
(19) Lloret, F.; De Munno, G.; Julve, M.; Cano, J.; Ruiz, R.; Caneschi, A. *Angew. Chem., Int. Ed.* **1998**, *37*, 135−138.
(20) Fernández, I.; Ruiz, R.; Faus, J.; Julve, M.; Lloret, F.; Cano, J.; Ottenwaelder, X.; Journaux, Y.; Munoz, C. *Angew. Chem., Int. Ed.* **2001**, *40*, 3039−3042.
(21) Pardo, E.; Ruiz-Garcia, R.; Cano, J.; Ottenwaelder, X.; Lescouezec, R.; Journaux, Y.; Lloret, F.; Julve, M. *Dalton Trans.* **2008**, 2780−2805.
(22) Glaser, T.; Theil, H.; Heidemeier, M. *C. R. Chim.* **2008**, *11*, 1121−1136.
(23) Spielberg, E. T.; Fittipaldi, M.; Geibig, D.; Gatteschi, D.; Plass, W. *Inorg. Chim. Acta* **2010**, *363*, 4269−4276.
(24) Plaul, D.; Geibig, D.; Görls, H.; Plass, W. *Polyhedron* **2009**, *28*, 1982−1990.
(25) Bencini, A.; Ciofini, I.; Uytterhoeven, M. G. *Inorg. Chim. Acta* **1998**, *274*, 90−101.
(26) Mitra, S. *Prog. Inorg. Chem.* **1977**, *22*, 309−408.
(27) Kennedy, B. J.; Murray, K. S. *Inorg. Chem.* **1985**, *24*, 1552−1557.
(28) Miyasaka, H.; Clerac, R.; Wernsdorfer, W.; Lecren, L.; Bonhomme, C.; Sugiura, K.-i.; Yamashita, M. *Angew. Chem., Int. Ed.* **2004**, *43*, 2801−2805.
(29) Coulon, C.; Miyasaka, H.; Clérac, R. *Struct. Bond.* **2006**, *122*, 163−206.
(30) Clerac, R.; Miyasaka, H.; Yamashita, M.; Coulon, C. *J. Am. Chem. Soc.* **2002**, *124*, 12837−12844.
(31) Glaser, T.; Heidemeier, M.; Weyhermüller, T.; Hoffmann, R.-D.; Rupp, H.; Müller, P. *Angew. Chem., Int. Ed.* **2006**, *45*, 6033−6037.
(32) Glaser, T.; Heidemeier, M.; Krickemeyer, E.; Bögge, H.; Stammler, A.; Fröhlich, R.; Bill, E.; Schnack, J. *Inorg. Chem.* **2009**, *48*, 607−620.
(33) Krickemeyer, E.; Hoeke, V.; Stammler, A.; Bögge, H.; Schnack, J.; Glaser, T. *Z. Naturforsch.* **2010**, *65b*, 295−303.
(34) Lis, T. *Acta Crystallogr., Sect. B* **1980**, *36*, 2042−2046.
(35) Sessoli, R.; Gatteschi, D.; Caneschi, A.; Novak, M. A. *Nature* **1993**, *365*, 141−143.
(36) Sessoli, R.; Tsai, H. L.; Schake, A. R.; Wang, S. Y.; Vincent, J. B.; Folting, K.; Gatteschi, D.; Christou, G.; Hendrickson, D. N. *J. Am. Chem. Soc.* **1993**, *115*, 1804−1816.
(37) Milios, C. J.; Raptopoulou, C. P.; Terzis, A.; Lloret, F.; Vicente, R.; Perlepes, S. P.; Escuer, A. *Angew. Chem., Int. Ed.* **2004**, *43*, 210−212.

(38) Milios, C. J.; Inglis, R.; Bagai, R.; Wernsdorfer, W.; Collins, A.; Moggach, S.; Parsons, S.; Perlepes, S. P.; Christou, G.; Brechin, E. K. *Chem. Commun.* **2007**, 3476−3478.
(39) Milios, C. J.; Vinslava, A.; Whittaker, A. G.; Parsons, S.; Wernsdorfer, W.; Christou, G.; Perlepes, S. P.; Brechin, E. K. *Inorg. Chem.* **2006**, *45*, 5272−5274.
(40) Milios, C. J.; Vinslava, A.; Wernsdorfer, W.; Moggach, S.; Parsons, S.; Perlepes, S. P.; Christou, G.; Brechin, E. K. *J. Am. Chem. Soc.* **2007**, *129*, 2754−2755.
(41) Milios, C. J.; Inglis, R.; Vinslava, A.; Bagai, R.; Wernsdorfer, W.; Parsons, S.; Perlepes, S. P.; Christou, G.; Brechin, E. K. *J. Am. Chem. Soc.* **2007**, *129*, 12505−12511.
(42) Piligkos, S.; Bendix, J.; Milios, C. J.; Brechin, E. K. *Dalton Trans.* **2008**, 2277−2284.
(43) Rinehart, J. D.; Fang, M.; Evans, W. J.; Long, J. R. *Nat. Chem.* **2011**, *3*, 538−542.
(44) Rinehart, J. D.; Fang, M.; Evans, W. J.; Long, J. R. *J. Am. Chem. Soc.* **2011**, *133*, 14236−14239.
(45) Bencini, A.; Gatteschi, D. *Electron Paramagnetic Resonance of Exchanged Coupled Systems*; Springer-Verlag: Berlin, 1990.
(46) Freiherr, v.; Richthofen, C.-G.; Stammler, A.; Bögge, H.; Glaser, T. *Eur. J. Inorg. Chem.* **2011**, 49−52.
(47) Kleij, A. W. *Eur. J. Inorg. Chem.* **2009**, 193−205.
(48) Hernández-Molina, R.; Mederos, A. In *Comprehensive Coordination Chemistry II*; McCleverty, J. A., Meyer, T. J., Eds.; Elsevier, Ltd.: Oxford, 2004; Vol. *1*; pp 411−446.
(49) Lopez, J.; Liang, S.; Bu, X. R. *Tetrahedron Lett.* **1998**, *39*, 4199−4202.
(50) Janssen, K. B. M.; Laquierra, I.; Dehaen, W.; Parton, R. F.; Vankelecom, I. F. J.; Jacobs, P. A. *Tetrahedron: Asymmetry* **1997**, *8*, 3481−3487.
(51) Costes, J.-P.; Dahan, F.; Dupuis, A.; Laurant, J.-P. *Dalton Trans.* **1998**, 1307−1314.
(52) Kwiatkowski, E.; Kwiatkowski, M. *Inorg. Chim. Acta* **1984**, *82*, 101−109.
(53) Bu, X. R.; Jackson, C. R.; Van Derveer, D.; You, X. Z.; Meng, Q. J.; Wang, R. X. *Polyhedron* **1997**, *16*, 2991−3001.
(54) Kwiatkowski, M.; Kwiatkowski, E.; Olechnowicz, A.; Ho, D. M.; Deutsch, E. *Dalton Trans.* **1990**, 3063−3069.
(55) Kwiatkowski, M.; Kwiatkowski, E.; Olechnowicz, A.; Kosciuszkopanek, B.; Ho, D. M. *Pol. J. Chem.* **1994**, *68*, 85−92.
(56) Costes, J.-P.; Dahan, F. o.; Dupuis, A. *Inorg. Chem.* **2000**, *39*, 5994−6000.
(57) Dayagi, S.; Degani, Y. In *The Chemistry of the Carbon-Nitrogen Double Bond*; Patai, S., Ed.; Interscience Publishers: London, 1970; p 64.
(58) Böttcher, A.; Elias, H.; Eisenmann, B.; Hilms, E.; Huer, A.; Kniep, R.; Röhr, C. *Z. Naturforsch. B* **1994**, *49*, 1089−1100.
(59) Mukherjee, C.; Stammler, A.; Bögge, H.; Glaser, T. *Inorg. Chem.* **2009**, *48*, 9476−9484.
(60) Mukherjee, C.; Stammler, A.; Bögge, H.; Glaser, T. *Chem.—Eur. J.* **2010**, *16*, 10137−10149.
(61) Atkins, R.; Brewer, G.; Kokot, E.; Mockler, G. M.; Sinn, E. *Inorg. Chem.* **1985**, *24*, 127−134.
(62) Chong, J. H.; Sauer, M.; Patrick, B. O.; MacLachlan, M. J. *Org. Lett.* **2003**, *5*, 3823−3826.
(63) Riddle, J. A.; Bollinger, J. C.; Lee, D. *Angew. Chem., Int. Ed.* **2005**, *44*, 6689−6693.
(64) Suresh, P.; Varghese, B.; Varadarajan, T. K.; Viswanathan, B. *Acta Crystallogr., Sect. E* **2007**, *63*, o984−o986.
(65) Jiang, X.; Vieweger, M. C.; Bollinger, J. C.; Dragnea, B.; Lee, D. *Org. Lett.* **2007**, *9*, 3579−3582.
(66) Lim, Y.-K.; Jiang, X.; Bollinger, J. C.; Lee, D. *J. Mat. Chem.* **2007**, *17*, 1969−1980.
(67) Jiang, X.; Bollinger, J. C.; Lee, D. *J. Am. Chem. Soc.* **2006**, *128*, 11732−11733.
(68) Glaser, T.; Heidemeier, M.; Fröhlich, R. *C. R. Chim.* **2007**, *10*, 71−78.
(69) Ottenwaelder, X.; Cano, J.; Journaux, Y.; Riviere, E.; Brennan, C.; Nierlich, M.; Ruiz-Garcia, R. *Angew. Chem., Int. Ed.* **2004**, *43*, 850−852.
(70) Dul, M.-C.; Ottenwaelder, X.; Pardo, E.; Lescouezec, R.; Journaux, Y.; Chamoreau, L. M.; Ruiz-Garcia, R.; Cano, J.; Julve, M.; Lloret, F. *Inorg. Chem.* **2009**, *48*, 5244−5249.
(71) Sauer, M.; Yeung, C.; Chong, J. H.; Patrick, B. O.; MacLachlan, M. J. *J. Org. Chem.* **2006**, *71*, 775−788.
(72) Yelamaggad, C. V.; Achalkumar, A. S.; Shankar Rao, D. S.; Prasad, S. K. *J. Am. Chem. Soc.* **2004**, *126*, 6506−6507.
(73) Riddle, J. A.; Lathrop, S. P.; Bollinger, J. C.; Lee, D. *J. Am. Chem. Soc.* **2006**, *128*, 10986−10987.
(74) Yelamaggad, C. V.; Achalkumar, A. S.; Rao, D. S. S.; Prasad, S. K. *J. Org. Chem.* **2007**, *72*, 8308−8318.
(75) Suresh, P.; Srimurugan, S.; Babu, B.; Pati, H. N. *Tetrahedron: Asymmetry* **2007**, *18*, 2820−2827.
(76) Lim, Y.-K.; Wallace, S.; Bollinger, J. C.; Chen, X.; Lee, D. *Inorg. Chem.* **2007**, *46*, 1694−1703.
(77) Pahor, N. B.; Calligaris, M.; Delise, P.; Dodic, G.; Nardin, G.; Randaccio, L. *Dalton Trans.* **1976**, 2478−2483.
(78) Lippe, K.; Gerlach, D.; Kroke, E.; Wagler, J. r. *Organometallics* **2008**, *28*, 621−629.
(79) Dalla Cort, A.; Gasparrini, F.; Lunazzi, L.; Mandolini, L.; Mazzanti, A.; Pasquini, C.; Pierini, M.; Rompietti, R.; Schiaffino, L. *J. Org. Chem.* **2005**, *70*, 8877−8883.
(80) Boghaei, D. M.; Mohebi, S. *J. Chem. Res., Synop.* **2002**, 72−75.
(81) Alarcon, S. H.; Olivieri, A. C.; Gonzalez-Sierra, M. *J. Chem. Soc., Perkin Trans.* **1994**, 1067−1070.
(82) Claramunt, R. M.; López, C.; Santa María, M. D.; Sanz, D.; Elguero, J. *Prog. Nucl. Magn. Reson. Spectrosc.* **2006**, *49*, 169−206.
(83) Salman, S. R.; Lindon, J. C.; Farrant, R. D.; Carpenter, T. A. *Magn. Reson. Chem.* **1993**, *31*, 991−994.
(84) Belmonte, M. M.; Escudero-Adán, E. C.; Benet-Buchholz, J.; Haak, R. M.; Kleij, A. W. *Eur. J. Org. Chem.* **2010**, 4823−4831.
(85) Hoffmann, H. M. R.; Eggert, U.; Walenta, A.; Weineck, E.; Schomburg, D.; Wartchow, R.; Allen, F. H. *J. Org. Chem.* **1989**, *54*, 6096−6100.
(86) Allen, F. H.; Kennard, O.; Watson, D. G.; Brammer, L.; Orpen, A. G.; Taylor, R. *J. Chem. Soc., Perkin Trans.* **1987**, S1.
(87) Theil, H.; Fröhlich, R.; Glaser, T. *Z. Naturforsch.* **2009**, *64b*, 1633−1638.
(88) Bejan, E.; Fontenas, C.; Aït-Haddou, H.; Daran, J.-C.; Balavoine, G. G. A. *Eur. J. Org. Chem.* **1999**, 2485−2490.
(89) Zhuo, J.-C. *Magn. Reson. Chem.* **1997**, *35*, 432−440.
(90) Plaul, D.; Plass, W. *Inorg. Chim. Acta* **2011**, *374*, 341−349.
(91) Kimura, M.; Watson, W. H.; Nakayama, J. *J. Org. Chem.* **1980**, *45*, 3719−3721.
(92) Hopf, H.; Maas, G. *Angew. Chem., Int. Ed.* **1992**, *31*, 931−954.
(93) Maas, G.; Hopf, H. iIn *The Chemistry of Dienes and Polyenes*; Rappaport., Ed.; John Wiley and Sons Ltd: New York, 1997; Vol. *1*; p 927−977.
(94) Hopf, H. *Classics in Hydrocarbon Chemistry*; Wiley-VCH: New York, 2000.
(95) Gholami, M.; Tykwinski, R. R. *Chem. Rev.* **2006**, *106*, 4997−5027.
(96) Hopff, H.; Wick, A. K. *Helv. Chim. Acta* **1961**, *44*, 380−386.
(97) Weltin, E.; Gerson, F.; Murrell, J. N.; Heilbronner, E. *Helv. Chim. Acta* **1961**, *44*, 1400−1413.
(98) Marsh, W.; Dunitz, J. D. *Helv. Chim. Acta* **1975**, *58*, 707−712.
(99) Wilke, G. *Angew. Chem., Int. Ed.* **1988**, *27*, 185−206.
(100) Jones, P. G.; Bubenitschek, P.; Höpfner, T.; Hopf, H. *Acta Crystallogr., Sect. C* **1997**, *53*, 920−921.
(101) Stanger, A.; Ashkenazi, N.; Boese, R.; Bläser, D.; Stellberg, P. *Chem.—Eur. J.* **1997**, *3*, 208−211.
(102) Höpfner, T.; Jones, P. G.; Ahrens, B.; Dix, I.; Ernst, L.; Hopf, H. *Eur. J. Org. Chem.* **2003**, *2003*, 2596−2611.
(103) Shinozaki, S.; Hamura, T.; Ibusuki, Y.; Fujii, K.; Uekusa, H.; Suzuki, K. *Angew. Chem., Int. Ed.* **2010**, *49*, 3026−3029.
(104) Galasso, V. *J. Mol. Struct.* **1993**, *281*, 253−257.

(105) Iyoda, M.; Tanaka, S.; Nose, M.; Oda, M. *Chem. Commun.* **1983**, 1058−1059.
(106) Patra, A.; Wijsboom, Y. H.; Shimon, L. J. W.; Bendikov, M. *Angew. Chem., Int. Ed.* **2007**, *46*, 8814−8818.
(107) Samuel, B.; Snaith, R.; Summerford, C.; Wade, K. *J. Chem. Soc. A* **1970**, 2019−2022.
(108) Marvel, C. S.; Aspey, S. A.; Dudley, E. A. *J. Am. Chem. Soc.* **1956**, *78*, 4905−4909.
(109) Biradar, N. S.; Kulkarni, V. H. *Z. Anorg. Allg. Chem.* **1971**, *381*, 312−315.
(110) Wang, X.; Zhang, X. M.; Liu, H. X. *Polyhedron* **1995**, *14*, 293−296.
(111) Dabrowski, J.; Kamienska-Trela, K. *Spectrochim. Acta* **1966**, *22*, 211−220.
(112) Wolfbeis, O. S.; Ziegler, E. *Z. Naturforsch.* **1976**, *31b*, 1519−1525.
(113) García-Martín, M. G.; Gasch, C.; Gómez-Sánchez, A.; Diánez, M. J.; López Castro, A. *Carbonhydr. Res* **1987**, *162*, 181−197.
(114) Dabrowski, J.; Dabrowska, U. *Chem. Ber.* **1968**, *101*, 2365−2374.
(115) Taoufik, N.; Pappalardo, R. R.; Sánchez Marcos, E. *Chem. Phys. Lett.* **2000**, *323*, 400−406.
(116) Crawford, S. M. *Spectrochim. Acta* **1963**, *19*, 255−270.
(117) Bosnich, B. *J. Am. Chem. Soc.* **1968**, *90*, 627−632.
(118) Di Bella, S.; Fragala, I.; Ledoux, I.; Diaz-Garcia, M. A.; Marks, T. J. *J. Am. Chem. Soc.* **1997**, *119*, 9550−9557.
(119) Sheldrick, G. M. *SADABS*; University of Göttingen: Göttingen, Germany, 2003.
(120) Sheldrick, G. M. *Acta Crystallogr.* **2008**, *A64*, 112−122.